JOURNAL OF MATERIALS SCIENCE 10 (1975) 1802–1825

Review
Liquid-phase separation in glass-forming systems

P. F. JAMES
Department of Ceramics, Glasses and Polymers, University of Sheffield, Northumberland Road, Sheffield, UK

This review is concerned with the process of liquid-phase separation in glass-forming systems. In the first part a general account of phase equilibria is presented together with a discussion of the thermodynamic behaviour of systems exhibiting liquid–liquid immiscibility. The estimation of free energies from phase-boundary data and the location of the spinodal boundary are briefly considered. The origin of immiscibility in silicate solutions is discussed from a thermodynamic approach. The importance of association, particularly in silicate systems, is stressed. In the second part of the review, an outline of the theories of homogeneous nucleation and spinodal decomposition is given and a review of recent theoretical developments. The intersecting growth model is discussed and also the later-stage coarsening of both droplet and interconnected structures. The theories are compared with experimental results (including electron microscope and small-angle X-ray scattering data) for various systems. The effects of phase separation on crystallization processes in glasses and on the physical and chemical properties of glasses are outlined. Although the results considered are for oxide systems where sufficient data are available, much of the discussion is applicable to glass-forming systems in general.

1. Introduction

A wide variety of binary or multicomponent systems, both organic and inorganic, exhibit liquid–liquid immiscibility and tend to separate into two or more liquid phases over a well defined range of composition and temperature. The phenomenon has been known for many years in glass-forming oxide systems, particularly those based on silica and boric oxide. A classic study of immiscibility in silicate systems, including the binary silica–alkaline earth systems was made by Greig [1] in 1927. Much of the early work was concerned with stable immiscibility in which liquid separation occurs at temperatures above the liquidus. Glasses formed by cooling such melts have either a layered structure or a strongly opalescent appearance. A region of stable immiscibility in a system can, therefore, limit the useful region of glass formation [2]. In recent years detailed attention has been also given to metastable or sub-liquidus immiscibility, particularly with the widespread use of the electron microscope. Here it is often possible to cool the glass-forming liquid through the region of metastable immiscibility without visually detectable opalescence, since we are dealing with high viscosities and diffusion rates are slow, to below the glass transformation temperature range. A very fine-scale microphase separation can thus be "frozen in" comprising droplets of one glass distributed within another, which may only be observed by electron microscopy. In certain cases separation is not even detectable in the electron microscope but can be observed after further heat-treatment above the transformation range but below the immiscibility boundary.

Interest in metastable immiscibility has been stimulated by the discovery and development of glass-ceramics, materials made by the controlled crystallization of glasses [3, 4]. Thus it has been found that liquid separation is often the precursor to crystal nucleation and growth in certain glass-

© 1975 Chapman and Hall Ltd. Printed in Great Britain.

ceramic compositions and can profoundly influence the crystallization path of a system on the phase diagram [5]. Of more direct importance, metastable immiscibility has been known for many years to occur in the Na_2O–B_2O_3–SiO_2 system and is basic to the manufacture of "Vycor" type glasses. In this process one of the separated phases is leached out by acid treatment leaving a porous silica skeleton which may be compacted by sintering to produce a high silica glass.

The purpose of this review is to give an account of the mechanism of liquid separation in glass-forming melts. The main emphasis will be on the kinetics of separation, but it will also be necessary to discuss the thermodynamics of liquid–liquid immiscibility, which has an important bearing on the mechanism of separation. Most of the experimental results discussed will be from silicate and borate systems, which due to their technological importance, have been the most extensively studied. The information on immiscibility in glass-forming systems is extensive and it will not be possible to discuss each individual system. Also no attempt will be made to describe the experimental techniques in detail. Levin [5] has given a compilation of immiscibility data in oxide systems, and has reviewed possible structural interpretations of immiscibility data based on crystal chemical considerations – the reader is referred to the articles by Levin [5] and Galakhov and Varshal [6] for detailed discussion. Other useful general references on glass-forming systems and phase separation are Rawson [2], Cahn and Charles [7] Porai-Koshits [8] and Seward [9].

2. Thermodynamic aspects of liquid–liquid immiscibility

We begin with a brief account of phase equilibria in liquid-separating systems. This will form a basis for the later discussion of kinetics. The object is also to describe the information which can be obtained from phase diagrams and thermodynamic data. A brief review is included of present ideas on the origin of immiscibility in silicate systems.

2.1. Phase diagrams and free energy–composition relations

Schematic binary phase diagrams with two-liquid immiscibility regions are shown in Fig. 1. Fig. 1a illustrates both stable and metastable immiscibility. Here the liquidus exhibits a horizontal portion corresponding to the monotectic temperature, which divides the region of stable unmixing from the region of metastable unmixing where the equilibrium phases are crystalline. Examples of systems showing this behaviour are MgO–SiO_2, CaO–SiO_2 and PbO–B_2O_3. An entirely sub-liquidus immiscibility region is illustrated in Fig. 1b. Similar behaviour is found in such systems as BaO–, Li_2O– and Na_2O–SiO_2, and the binary alkali borates. Here a flattening of the liquidus or pronounced "S" shape is often an indication of the presence of metastable immiscibility.

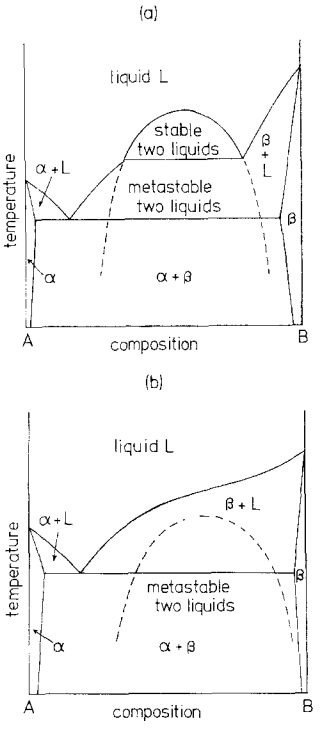

Figure 1 Schematic binary phase diagrams showing (a) both stable and metastable two-liquid immiscibility and (b) entirely sub-liquidus metastable immiscibility.

Schematic Gibbs free energy versus composition curves for a binary system A–B above and below the upper consolute temperature T_c of an immiscibility dome are shown in Fig. 2. The presence of crystalline phases is ignored since we are concerned here with either stable or metastable liquid–liquid equilibria. At temperature T_2 initial compositions between *a* and *b* will separate into two liquids with compositions given by the common tangent construction. The equilibrium condition is that the chemical potential of component A is equal in the two phases, and similarly for component B. The variation of the equilibrium compositions with temperature determines the *binodal* or equilibrium curve. The loci of the

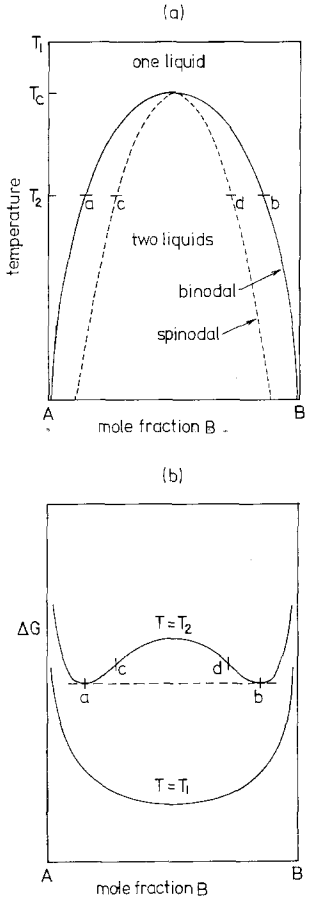

Figure 2 (a) Schematic two-liquid immiscibility region showing binodal and spinodal. (b) Corresponding free energy curves versus composition x (mole fraction of component B) for temperatures T_1 and T_2.

points of inflexion in the free energy curves, where $\partial^2 \Delta G/\partial x^2 = 0$, give the *spinodal* boundary. The importance of the spinodal in relation to the mechanism of phase separation will be considered later.

The general features of liquid–liquid immiscibility can be discussed qualitatively in terms of a simple statistical model in which atoms A and B are randomly mixed on a regular lattice [10]. In this model, which is only a crude approximation to a liquid solution, the free energy of mixing may be expressed as

$$\Delta G = \Delta H - T\Delta S$$
$$= \alpha x(1-x) + RT[x \ln x + (1-x)\ln(1-x)], \quad (1)$$

where x is the mole fraction of B and α is given by

$$\alpha = NZ[E_{AB} - \tfrac{1}{2}(E_{AA} + E_{BB})] \quad (2)$$

where E_{AA}, E_{BB} and E_{AB} are the energies of the various bonds between atoms, Z is the number of nearest neighbours surrounding each atom and N is Avogadro's number.

This is essentially the regular solution model, originally introduced by Hildebrand [11], in which the entropy of mixing ΔS is that of an ideal solution. It is easily shown that α is related to the upper consolute temperature by $\alpha = 2RT_c$. For immiscibility to occur α (and hence ΔH) must be positive. The free energy curves are symmetrical about $x = 0.5$ and are similar to those in Fig. 2. The binodal and spinodal curves [12] are also symmetrical about $x = 0.5$.

This model is useful in discussing some metallic systems [13] but in the above form has limited value when applied to silicate and other oxide melts, which are more complex than a simple random mixture of atoms. Moreover, the observed immiscibility domes in these systems are often far from symmetrical (Fig. 3). For example, in the binary lithia- and soda-silica systems the critical composition occurs at a mole fraction of alkali oxide of about 0.1 rather than 0.5. The non-regular mixing is also confirmed by available thermodynamic data. Charles [14] has estimated

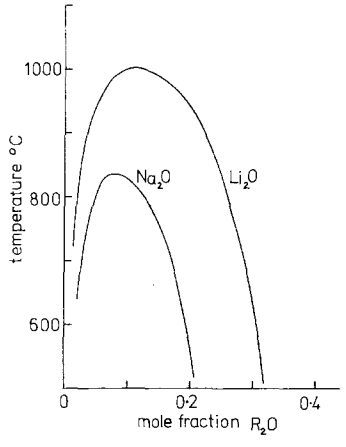

Figure 3 Sub-liquidus immiscibility regions in soda–silica and lithia–silica systems, based on published data [15–18].

activities, and hence free energies of mixing, in the Li_2O–, Na_2O– and K_2O–SiO_2 systems using published liquidus, volatility and cell potential data. The ΔG curves are highly asymmetrical when plotted against the mole fraction of alkali oxide. The general behaviour is illustrated schematically

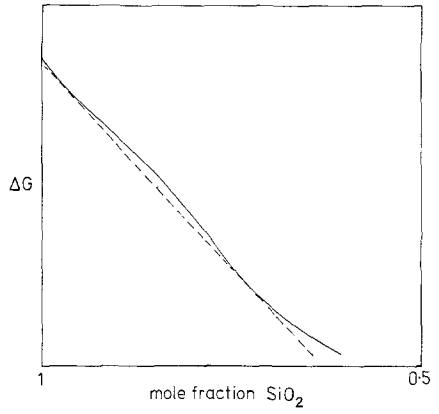

Figure 4 Schematic free energy versus composition curve to illustrate real (non-regular) behaviour in a binary silicate system.

in Fig. 4. Again the common tangent may be drawn which touches the curve at two points corresponding to the equilibrium compositions of the separating phases.

Owing mainly to the considerable experimental difficulties involved, there is a general lack of accurate activity and free energy data in glass forming oxide systems. Such data are required for a detailed quantitative test of theories of liquid separation kinetics – it enables the thermodynamic driving force to be calculated and the position of the spinodal curve to be located. A method of obtaining free energy data if no direct measurements are available is to use an empirical solution model or free energy expression and obtain a fit to the experimental binodal curve.

Hammel [18] and Burnett [19] have applied this method to silicate systems. Burnett [19] employed a sub-regular solution model, the properties of which have been discussed by Hardy [20]. The free energy is as in equation 1 except that the enthalpy is now represented by

$$\Delta H = (A_1 + A_2 x)x(1-x), \qquad (3)$$

where A_1 and A_2 are adjustable parameters which are determined from the phase-boundary data. Burnett found that this model provides a simple and useful means of estimating the position of the spinodal curve, which may be derived using the condition that $\partial^2 \Delta G/\partial x^2 = 0$. Hammel [18] has used another two parameter model, the Lumsden model [21] to estimate approximate free energies in the soda–lime–silica system for his kinetic studies of liquid separation.

A logical extension of the sub-regular model is to expand ΔH, or more generally the excess free energy over ideal behaviour, as a polynomial in x incorporating a series of adjustable parameters. In principle this would seem to be a powerful method of obtaining free energy data from miscibility gap data.

Van der Toorn and Tiedema [22] have proposed such a multi-parameter model. However, in practice it has been found that considerable errors may be incurred in the application of the Van der Toorn and Tiedema model to the estimation of free energy curves [23]. An attempt [19] to apply the same method to phase-boundary data in silicate systems using a computer was unsuccessful due to the extreme sensitivity of the model to small shifts in the phase boundary.

Cook and Hilliard [24] describe a simple method of estimating the spinodal which may be preferable even when thermodynamic data are available. If x, x_s and x_c are the equilibrium, spinodal and critical compositions respectively then it can be shown, using a Taylor expansion of the free energy in T and x about the critical point that

$$x_s - x_c = (x - x_c)/\sqrt{3} \qquad (4)$$

This equation is exact for the limit $T \to T_c$ and is a good approximation down to $T/T_c \sim 0.9$. For an asymmetric miscibility gap the two sides of the gap are treated separately in the calculation.

It can also be shown using a Taylor expansion [19] that near the critical point

$$|x - x_c| \propto |T - T_c|^{\frac{1}{2}}. \qquad (5)$$

This relation is confirmed experimentally in a number of binary silicate systems [19, 25].

2.2. The origins of immiscibility

Various attempts have been made to explain the extent of the immiscibility region in silicate and borate systems in terms of the co-ordination of oxygen ions around metal cations and the strength of the ionic bonds between the cations and their oxygen neighbours [26–28]. As Rawson [29] has pointed out in most of these discussions there is no explicit recognition that immiscibility is essentially a thermodynamic phenomenon.

Recently Charles [30] has given a useful thermodynamic analysis of the origin of immiscibility in silicate solutions by considering both the entropy and enthalpy contributions to the free energy. Charles shows that a more realistic estimate of the entropy of mixing than the assump-

tion of ideal mixing of SiO_2 and metal oxide may be obtained by considering a statistical model involving the interchange of bridging and non-bridging oxygen ions over the available sites. Here "bridging" oxygens refer to those linked to two silicons and "non-bridging" oxygens refer to those linked directly to only one silicon. It is assumed also that the non-bridging oxygen ions occur in pairs. The entropy of mixing per mole of solution ΔS is then given by

$$\frac{\Delta S}{R} = x \ln \left\{ \frac{2(1-x)}{x} \right\} + (2-3x) \ln \left\{ \frac{2(1-x)}{2-3x} \right\}, \quad (6)$$

where x is the mole fraction of M_2O or MO.

The presence of free oxygen ions O^{2-}, which reach an appreciable concentration for higher mole fractions of metal oxide can also be taken into account but the above expression appears to be a good approximation up to $x = 0.5$.

According to Charles, the heat of mixing may be considered in two parts; an exothermic contribution resulting from the conversion of bridging Si–O bonds to non-bridging Si–O bonds, and an endothermic contribution arising from the difference in coulombic interaction energy between metal cations and free oxygen ions in the pure metal oxide and the coulombic interaction energy between metal cations and non-bridging oxygen ions in the melt.

For the binary transition metal oxide systems MnO– and $FeO–SiO_2$, Charles shows, from an analysis of available thermodynamic data, that the enthalpy of formation of the solution is positive (endothermic) over most of the composition range, which may be attributed to the fact that the endothermic contribution mentioned above outweighs the exothermic contribution. This agrees with a description of the origin of immiscibility in these systems given by Richardson [31] – the competition between the entropy term and the endothermic enthalpy term leads at some temperature to immiscibility – i.e. a reduction in the total free energy by separation into two phases. This picture is also qualitatively similar to the simple description of immiscibility given by the regular solution model – in which the parameter α is positive (positive ΔH).

However, Charles shows that this explanation of immiscibility does not hold in the alkali and alkaline earth silica systems. Experimentally the heat of mixing of silica rich solutions of these systems are exothermic and not endothermic as in MnO– and $FeO–SiO_2$, probably because the exothermic contribution due to the conversion of bridging to non-bridging Si–O bonds now predominates over the endothermic contribution mentioned earlier. On the other hand, for the silica rich regions of these systems the partial molar heat of solution of silica, ΔH_{SiO_2}, is positive, whilst that of the metal oxide, ΔH_{MO}, is negative (the total heat of mixing $\Delta H = x\Delta H_{MO} + (1-x)\Delta H_{SiO_2}$ and also $\Delta H_{SiO_2} = \Delta H - x\partial\Delta H/\partial x$).

It is this positive ΔH_{SiO_2} which accounts for the immiscibility since when the entropy and enthalpy contributions to the free energy are added, the free energy curve exhibits a small deviation in curvature or "hump" similar to that shown schematically in Fig. 4. It is worth noting that in practice the free energy changes involved in immiscibility are often very small compared with the overall free energies of mixing. There has been a tendency frequently to exaggerate the free energy changes when drawing schematic free energy curves.

Charles attributes the positive ΔH_{SiO_2} to a decrease in solution of the bond angles of the bridging bonds (i.e. the angles between neighbouring silica tetrahedra) – this process being associated with a contraction in volume. This explanation of immiscibility, therefore, depends on the chain-like character of the network forming species of the silica solutions, unlike the description used for the transition metal oxide systems, although the chain-like or polymeric species may also play an important role even for these systems.

In spite of the importance to the thermodynamics of immiscibility very little is known about the polymeric or associated character of silicate melts. It has been suggested that, depending on the percentage of metal oxide present, silicate melts contain silicate anions of varying size and complexity (see for example [32]). If sufficient metal oxide is present the silica will occur predominantly as SiO_4^{4-}. As the silica content is increased a series of polycondensation reactions may be envisaged such as

$$SiO_4^{4-} + SiO_4^{4-} \longrightarrow Si_2O_7^{6-} + O^{2-}$$

$$SiO_4^{4-} + Si_2O_7^{6-} \longrightarrow Si_3O_{10}^{8-} + O^{2-} \text{ etc.}$$

These silicate anions can form, in principle, various configurations including chains, rings and

sheets and in this view we may regard liquid silicates as condensation polymers derived from the monomer SiO_4^{4-}. This approach has been used by Masson [33] and others to discuss the thermodynamics of the metal oxide rich compositions of these systems, but so far little attempt has been made to apply a more realistic structural model to the silica-rich compositions where immiscibility may occur. Burnett [19] has discussed the application of the associated solution model developed by Prigogine and others [34] to silicate solutions. In this model complexes of A_i are considered to form from i monomers of A in a mixture of the components A and B. In applying the model Burnett regarded A as silica and B as metal oxide. By considering the complexes to be in thermodynamic equilibrium with the monomers and also that the mixture of monomers and complexes behave ideally, expressions for the activities and free energy can be derived. The important result of the calculation is that association can give rise to phase separation. From the point of view of theory this, or a similar approach, seems promising and would merit further development.

We have already mentioned the inadequacies of the regular solution model in explaining the highly asymmetric miscibility gaps in many binary silicate systems, when the data are plotted in terms of the mole fraction of SiO_2 or metal oxide. Haller *et al.* [17] have recently proposed a modification of the regular model which considers the regular mixing of new end components – a complex molecule or "multimer" $(SiO_2)_m$ and a stoichiometric compound $R_2O.nSiO_2$ at the limit of the miscibility gap on the alkali oxide side, where m and n are integers. A similar approach was also previously suggested by Moriya [35]. Haller *et al.* chose appropriate values of m, n and a parameter ΔS (representing the additional entropy change due to changes in internal degrees of freedom of the liquids on mixing) to produce a symmetric gap when the experimental miscibility boundary data were plotted in terms of the mole fractions of the new end components. For soda–silica an excellent fit was obtained with $m = 8$ and $n = 3$, representing the end components $(SiO_2)_8$ and $Na_2O.3SiO_2$. Similarly, for lithia–silica the required values were $m = 6$, $n = 2$, and for baria–silica $m = 8$, $n = 2$. Haller *et al.* point out that the formulae of the end members do not necessarily represent the structural units in the melt and that multiplication of both end members by an integer gives an equally acceptable result. In fact the complex multimer $(SiO_2)_{24}$ represents the lowest common denominator for the two alkali silicate systems. This would imply that at the same time the structural units in the other liquids are $4(Li_2O.2SiO_2)$ and $3(Na_2O.3SiO_2)$. Haller *et al.* cite supporting evidence from crystal structure data [36] for the compound $Li_2O.2SiO_2$, which has a four membered structure $Li_8Si_8O_{20}$ per unit cell.

The above analysis has been applied by Macedo and Simmons [37] to the miscibility gaps in various binary borate systems containing K_2O, Li_2O, Rb_2O, Cs_2O and PbO using the experimental data of Shaw and Uhlmann [38], and Simmons [39]. Excellent agreement with the data was obtained by considering the regular mixing of an appropriate stoichiometric compound depending on the system (such as $K_2O.3B_2O_3$) and a complex boron trioxide end member $(B_2O_3)_5$, the latter component being the same for all the systems.

The existence of complex structural groups such as $(SiO_2)_{24}$ and $(B_2O_3)_5$ in silicate and borate glasses is an interesting possibility but has yet no independent confirmation.

To conclude this section, the thermodynamic evidence we have discussed emphasizes the importance of the associated or polymeric nature of the systems. However, at present it is not clear how far the several approaches described are consistent with one another, and a great deal of further work is required before the origin of immiscibility in silicate and other systems is completely established. Further development of theories based on concepts such as association and accumulation of experimental thermodynamic data may help to understand not only the origin of immiscibility but also the nature of the chemical species and interactions occurring in the solutions.

3. Kinetics of phase separation in glass-forming melts

It is appropriate to present an outline of the theories of phase separation kinetics and an indication of recent theoretical developments, before discussing the experimental results for glass systems in detail. Excellent general reviews of the theory are contained in [40–43].

We begin by considering a schematic free energy–composition diagram for a phase-separating system at a temperature below the

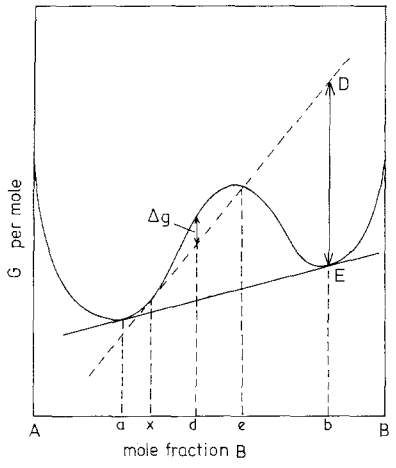

Figure 5 Schematic free energy-composition diagram for $T < T_c$ showing graphical method of determining the thermodynamic driving force for liquid-phase separation.

upper consolute temperature (Fig. 5). The equilibrium compositions of the separating phases are a and b. First consider the case where the initial composition is at x, and a small region of the equilibrium composition b separates out. It can be shown [40] that, neglecting interfacial effects, the free energy decrease per mole of the separating phase is given graphically by the distance DE, which is the height above the free energy curve at composition b of the tangent drawn to the curve at the initial composition x. This is the overall driving force for separation of the equilibrium phase. For a small region (or fluctuation) of composition d to separate the driving force is again the difference between the tangent and the free energy curve at d. However, now there is an increase in free energy per mole (Δg). Clearly a fluctuation must exceed the composition e before the free energy will decrease and the driving force is positive. There is thus a thermodynamic barrier to overcome before phase separation will occur. If x lies between a and the point of inflexion on the curve the system is *metastable* to infinitesimal compositional fluctuations. This corresponds to the region between the binodal and spinodal curves often referred to as the region of "nucleation and growth". However, if the initial composition x lies just to the right of the inflexion point (at d for example), for a small fluctuation the free energy change is negative and there is no thermodynamic barrier. Between the points of inflexion the system is *unstable* to infinitesimal fluctuations of composition and separation can occur with a continuous fall in free energy, there being no barrier other than that of diffusion. This corresponds to the region inside the spinodal and the process is called "spinodal decomposition".

Regardless of the mechanism involved the end result of separation will be the equilibrium phases a and b, the relative proportions being determined by the well known Lever Rule.

It is convenient to consider the kinetics in two stages – the early stage of the transformation and the later stage when the transformation is approaching completion. For simplicity we will discuss only two-component systems.

3.1. Theories of the initial stage of phase separation

3.1.1. Classical homogeneous nucleation

One approach is to consider the formation of discrete nuclei of the equilibrium composition at b (Fig. 5) from the initial composition x. It is assumed that the nucleus is uniform and that the boundary between nucleus and matrix is sharp with an associated interfacial free energy σ. Classical theory [40–42] predicts that stable nuclei, which can grow, have a radius greater than the critical value r^* equal to $2\sigma/\Delta G_v$ where ΔG_v is the free energy change per unit volume of phase transformed. The number of critical nuclei formed per unit volume per second is given by the expression of the form

$$I = K_v \exp -(\Delta G_D + W^*)/kT, \qquad (7)$$

where W^*, the free energy to form a critical nucleus, is given by $K\sigma^3/\Delta G_v^2$ (K is a geometrical constant dependent on nucleus shape); ΔG_D is the activation energy for transport across the interface and K_v is essentially constant [40].

The temperature dependence of I is shown schematically in Fig. 6. A range of no detectable nucleation is predicted just below the miscibility temperature, T_m, although the rate of growth of the separated phase is not zero. Both nucleation and growth rates decrease rapidly at high undercoolings due to the decrease in diffusion rates, and increase in viscosity.

The classical theory is more readily applied quantitatively to the case where no change of composition occurs, as for example in crystallization in a one component system. For a two component system ΔG_v can only be estimated from the driving force (Fig. 5) if detailed free energy – composition data are available. Also in general σ and ΔG_D will vary with composition and temperature.

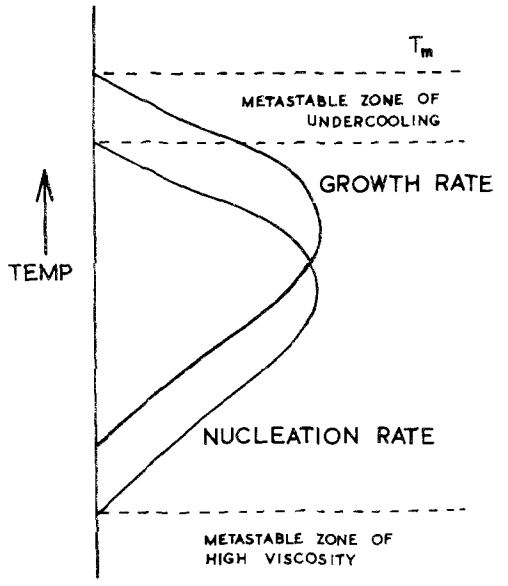

Figure 6 Schematic variation with temperature of homogeneous nucleation rate I and growth "rate" of second phase (strictly for early stage growth, and coarsening, the particle radius is a function of temperature and time – see Section 3.2 and [18, 25].

From the introductory discussion, nucleation (whether classical or not) is most likely to apply outside the spinodal and close to the binodal. However, it may be remarked that a nucleation mechanism could, in principle, occur even within the spinodal region.

3.1.2. Theory of Cahn and Hilliard

Objections to the above theory as applied to separation in a miscibility gap include the assumptions that the nucleus is uniform and has the composition of the equilibrium separating phase. Cahn and Hilliard [44] have developed a more comprehensive approach which considers the free energy of a system having a spatial variation of composition. This approach does not require the assumption of an uniform nucleus and the separation of the free energy into volume and surface contributions. The local Helmholtz free energy per unit volume, f, is expressed as a function of the local composition c (the mole fraction of component B in the binary solution) and the composition derivatives of the immediate environment, and may be expanded in a Taylor series about $f(c)$ the free energy per unit volume of solution of uniform composition c. The total free energy is of the form

$$F = \int_v [f(c) + \kappa(\nabla c)^2 + \ldots] \, dV. \qquad (8)$$

The term $\kappa(\nabla c)^2$, the first term in the expansion, represents the increase in free energy due to the gradient of composition and may be associated with the energy to form an interface. For convenience the composition is here denoted by c and not x since c is used consistently in most of the literature. Cahn and Hilliard use the more correct Helmholtz free energy F and not G in their analysis. However, in condensed systems at 1 atm pressure the difference between F and G can be ignored.

From the above expression Cahn and Hilliard derived the properties of the critical nucleus in the metastable region. At very low supersaturations the properties of the nucleus were found to approach those of the classical theory; but as supersaturation increases the work of formation of the critical nucleus W^* becomes progressively less than given classically and approaches continuously to zero at the spinodal. Also the interface of the nucleus becomes more diffuse and the composition at the centre of the nucleus approaches that of the matrix.

3.1.3. Spinodal decomposition

So far we have discussed the case where the composition changes are large in degree but small in extent (nucleation). The second limiting case (as formulated by Gibbs [45]) is a compositional change small in degree but large in extent. Spontaneous decomposition inside the spinodal has been treated by Hillert [46] and Cahn [47]. The analysis of Cahn was based on Equation 8 using only the first term $\kappa(\nabla c)^2$ in the expansion. It was assumed that higher order gradient energy terms could be neglected, since only the initial stages of phase separation were considered. Cahn found that inside the spinodal the system is unstable to infinitesimal sinusoidal fluctuations of wavelengths greater than a critical value λ_c (or $2\pi/\beta_c$), given by

$$\lambda_c = (-8\pi^2\kappa/f'')^{\frac{1}{2}}, \qquad (9)$$

where $f'' = \partial^2 f/\partial c^2$. As the spinodal is approached ($f'' \to 0$), λ_c tends to infinity.

To treat the kinetics of spinodal decomposition it is necessary to solve a general diffusion equation in which all terms not linear in c are neglected,

$$\partial c/\partial t = Mf''\nabla^2 c - 2M\kappa\nabla^4 c \qquad (10)$$

where M is the mobility. This linearized equation holds for an isotropic system without strain energy

and thus applies to the viscous liquids or glasses under consideration.

A general solution for the composition as a function of time can be expressed in a Fourier series with components of the form

$$c(\mathbf{r}, t) - c_0 = A(\boldsymbol{\beta}, t) \exp(i\boldsymbol{\beta}.\mathbf{r}) \quad (11)$$

where

$$A(\boldsymbol{\beta}, t) = A(\boldsymbol{\beta}, 0) \exp(R(\beta)t). \quad (12)$$

Here c_0 is the average composition, $\mathbf{r}$ a position vector, $A(\boldsymbol{\beta}, t)$ is the amplitude of the Fourier component of wave vector $\boldsymbol{\beta}$ at time t, $A(\boldsymbol{\beta}, 0)$ the amplitude at $t = 0$ and $R(\beta)$ is an amplification factor given by

$$R(\beta) = -Mf''\beta^2 - 2M\kappa\beta^4. \quad (13)$$

$R(\beta)$ is positive in the spinodal region but only for wavenumbers less than β_c (Fig. 7). The maximum amplification occurs at $\beta = \beta_c/\sqrt{2}$. Owing to the

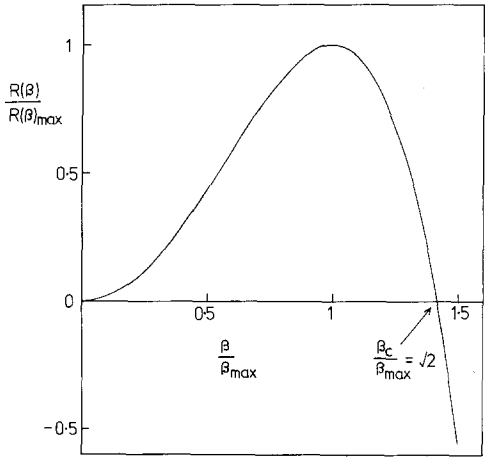

Figure 7 Amplification factor $R(\beta)$ in Cahn's theory versus wavenumber β.

sharpness of the peak this particular wavenumber will grow most rapidly in amplitude and will dominate the others. Hence only the wavenumber β_m was considered in Cahn's treatment and at a finite time after the transformation has begun the composition in the system will be describable by a superposition of sine waves of fixed wavelength but random in orientation, phase and amplitude. Cahn [48] has constructed a mathematical model of the separation process using a computer to produce sections through the two-phase structure. The striking interconnectivity of the phases strongly resembles micrographs of phase-separated glasses (Fig. 8), and we will return to this point later. The nucleation and growth and spinodal mechanisms may be compared for isothermal

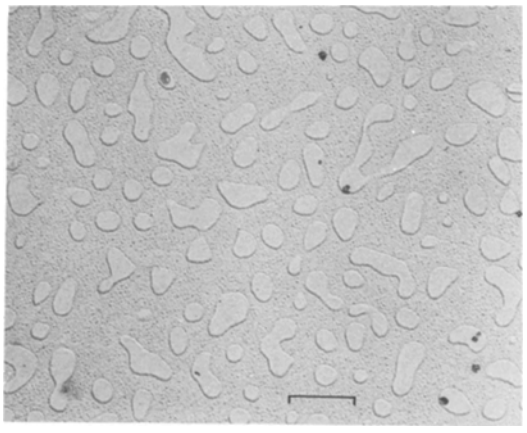

Figure 8 Replica electron micrograph of 85 SiO_2–10 Na_2O–5 CaO mol% glass heat-treated at 795° C for 2 h. Marker indicates 0.5 μm. Note "background" structure in matrix due to fine scale secondary phase separation during cooling [19].

separation. For nucleation and growth there is an invariance of second phase composition with time, the interface between phases is always the same degree of sharpness during growth and there is a tendency for separation of spherical particles with low connectivity. For spinodal decomposition there is a continuous variation of both extremes in composition until the equilibrium compositions are reached, the interface is initially diffuse but eventually sharpens and there is a tendency for high connectivity in the second phase. The contrast between the two mechanisms is illustrated in Fig. 9.

Cahn and Charles [7] have discussed the kinetics of spinodal decomposition with particular reference to liquid separation in glasses. One version of the kinetics (considered above) is for a quench from the single phase region followed by isothermal holding at a temperature below the spinodal. The most rapid increase in the amplitude

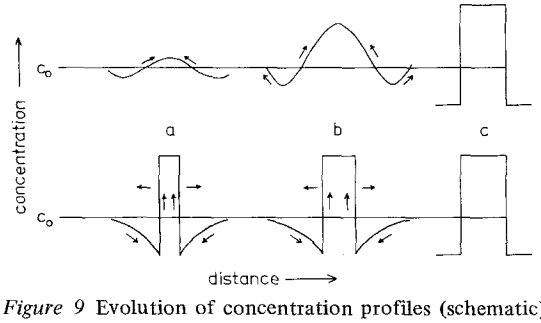

Figure 9 Evolution of concentration profiles (schematic) for spinodal decomposition (top) and nucleation and growth (bottom) from early stage (a) to final stage (c). c_0 is the average composition. Modified after Cahn [48].

of the fluctuations (typically 30 to 100 Å in wavelength) should occur for an undercooling ΔT below the spinodal which is about 10% of the spinodal temperature. Under these conditions the decomposition can be very rapid, even in fairly viscous liquids, and will occur in a time of considerably less than 1 sec. However, at lower temperatures diffusion rates will become so slow as to inhibit phase separation. The other version of the kinetics, which is more applicable in practice, is for a continuous quench from the single phase region. To avoid separation entirely, an estimated cooling rate of $1^\circ C\,sec^{-1}$ is required if the diffusion coefficient D is $10^{-19} m^2 sec^{-1}$ at the temperature where the rate is a maximum, and $1000^\circ C\,sec^{-1}$ is required if D is $10^{-16} m^2 sec^{-1}$.

3.1.4. Recent developments in spinodal decomposition theory

The theory we have outlined is only applicable in the very early stages of decomposition. Thus it is assumed that f'' is constant or equivalently that the free energy is a parabolic function of composition. This would indicate that the system could decrease its free energy indefinitely and clearly the approximation becomes progressively worse in the later stages of decomposition when the equilibrium compositions are being approached (Fig. 2b). Treatment of the later stages of decomposition, therefore, requires the use of a more realistic free energy relation. It is also necessary to consider the dependence of M and κ on composition. Analytical [49] and numerical [50] solutions of the non-linearized diffusion equation show that the effects of these modifications to the theory include a limitation in the amplitude of growth and a sharpening of the interfaces between phases.

A weakness of the linearized theory [52] is that the amplitude of Fourier components with $R(\beta)$ negative should decay to zero (Equation 12) whereas in fact they must slow down and gradually approach the equilibrium non-zero amplitude due to thermal fluctuations. This would decrease the amplification factor and hence could provide an explanation for the curvature in some experimental plots of $R(\beta)/\beta^2$ versus β^2 (see later). Cook [51] has confirmed this point in an important modification to Cahn's theory, in which the influence of random thermal composition fluctuations (analogous to Brownian motion) were considered by adding a random flux term to the diffusion equation.

Recently, Hopper and Uhlmann [53] have extended the thermodynamics of non-uniform systems to include various higher derivative terms not present in the Cahn and Hilliard treatment (see Equation 8). They investigated the relative importance of the terms using a mean field pair interaction (MFPI) analysis and also the effects of two of the higher derivative terms on the profile and interfacial tension of a diffuse interface. In a subsequent paper [54] the effects of the higher order terms on spinodal decomposition were discussed. The inclusion of the next order term was found to have little effect on the formalism of the early stage kinetics except for a modification of the amplification factor $R(\beta)$ in the usual formulation. However, problems were encountered in attempting to extend the analysis to include still higher terms. Hopper and Uhlmann have also developed a formulation of spinodal decomposition based on a MFPI theory which avoids the use of diffuse interface theory entirely and analyses decomposition directly in terms of pair interactions [55, 56]. Comparison of this and other treatments with experiment will be considered below.

3.1.5. Intersecting growth theory of Haller

Following the work of Cahn, the highly interconnected microstructure of many phase-separated glasses observed by electron microscopy was taken by some authors as evidence for spinodal decomposition in these glasses. However, it is now realized that the morphology alone is not sufficient to decide on the mechanism of separation. Thus Haller [57] has demonstrated that an interconnected microstructure can also be produced by classical nucleation, to form a high density of small discrete spherical particles, followed by radial growth of these particles until impingements occur. The high degree of interconnectivity possible with such a mechanism is illustrated by the fact that for an occupied volume of the spheres of 50%, each sphere on average intersects 5.5 others and only 0.4% of the spheres remain unattached; for an occupied volume of $33\frac{1}{3}$% each sphere on average intersects 3.2 others and only 4% are unattached.

An objection to this model may be raised [58] on the grounds that during growth each particle is surrounded by a depleted diffusional zone. When two such zones begin to overlap, growth progress-

ively slows down and the spheres are prevented from making contact. Counter arguments have been advanced to overcome this objection [59, 60]. It has been suggested [60] that the classic boundary concept of diffusion is no longer applicable to bodies of small magnitudes and has to be replaced by the concept of a transitional fluctuating boundary. From ultrasonic and electron microscope evidence it is estimated that the fluctuations are of the order of 10 to 50 Å. Thus when the particles reach a separation of this order they effectively touch and neck formation may occur with eventual coalescence. The larger the nucleation density the closer the spherical particles will approach each other before matrix depletion slows down the diffusion process. Hence in systems having almost equal volume fractions a high nucleation density may produce a highly interconnected microstructure whereas a low nucleation density may produce isolated droplets and low interconnectivity. Another possible mechanism of particle coalescence involves the Brownian motion of the second phase particles [59]. A detailed discussion of various coalescence models has been given [61]. The intersecting growth model has received support particularly from the experimental work of Seward *et al.* [59], as will be seen later.

3.2. Theories of the later, coarsening stage of phase separation

Consider the early stage of growth of a distribution of isolated spherical droplets produced by nucleation in the metastable region of the miscibility gap. Initially the matrix phase will be highly supersaturated. Thus the droplets will grow by long range diffusion and at constant temperature a parabolic relation $\bar{r}^2 \propto t$ is expected, where $\bar{r}$ is the average droplet radius. At a later stage of growth when the matrix is approaching its equilibrium composition a coarsening process begins to dominate, in which the smaller particles tend to dissolve and the larger particles to grow at their expense.This preferential growth of the larger particles is driven by the overall decrease in interfacial free energy and analysis [62–65] shows that for growth controlled by long range diffusion the mean radius should increase with time according to

$$\bar{r}^3 - \bar{r}_0^3 = (8/9)(\sigma/RT)DC_\infty V_m^2 t, \quad (14)$$

where $\bar{r}_0$ is the mean radius at the onset of coarsening, σ the interfacial free energy, D the effective diffusion coefficient, C_∞ the equilibrium concentration of "solute" in the matrix (mol m^{-3}) and V_m the molar volume of the droplet phase. The theory also predicts that the number of particles per unit volume N_v is proportional to $1/t$ and that the size distribution of particles is a well defined universal function of $r/\bar{r}$. It is interesting to note that if the coarsening process is controlled by a surface reaction rate and not by long range diffusion, $\bar{r}^2 \propto t$ and $N_v \propto t^{-3/2}$.

The coarsening of a highly interconnected two phase system in which the volume fractions remain constant has been treated by Haller [57]. Where mass transport across the interfaces is rapid and volume diffusion is the rate controlling process the total interfacial area in the system is given by $S_T \propto t^{-1/3}$. The mechanism is similar to the coarsening of isolated droplets described above except that here the process involves mass transport from convex to concave interfaces. For interface control Haller found $S_T \propto t^{-1/2}$.

3.3. Experimental evidence

3.3.1. Earlier investigations

Among the earliest systematic studies of the kinetics of phase separation were those of Ohlberg and co-workers [66–69], Haller [57] and Moriya *et al.* [15]. Ohlberg *et al.* [67] studied the growth rate of the silica rich droplets in a 76 SiO_2–13 Na_2O–11 CaO (mol %) glass using replica electron microscopy and found that the average radius of the droplets was proportional to $t^{1/2}$, indicating long-range diffusional control.

This result was confirmed by comparison of light scattering data with the theory of scattering for diffusion controlled phase separation [70]. Also light scattering measurements made on a 22 CaO–14 Al_2O_3–10 B_2O_3–54 SiO_2 glass [69] indicated the presence of composition gradients around the growing particles in agreement with diffusion controlled growth theory. It is now clear that these studies were concerned with the initial growth of the droplets before the onset of coarsening.

Moriya *et al.* [15] studied the morphology and kinetics of separation in several binary and ternary alkali silicate glasses using electron microscopy of both surface carbon replicas and thin glass specimens. In these glasses the initial stage of separation occurred very rapidly at the temperatures used. As a result only the later stage coarsening process was

observed. The average radius of particles $\bar{r}$ was proportion to $t^{1/3}$ in agreement with the theory of diffusion controlled coarsening (Section 3.2). Microstructures ranging from isolated droplets to highly interconnected phases were found but little could be inferred about the initial mechanism of separation.

3.3.2. Studies of later stage coarsening.

McCurrie and Douglas [71] have made a thorough quantitative study of the coarsening of droplets in a 1 K_2O–26 Li_2O–73 SiO_2 composition. Surface carbon replicas of fractured and etched specimens were examined by electron microscopy and various parameters including mean radius $\bar{r}$, number of particles per unit volume N_v, total surface area per unit volume S_T and volume fraction of dispersed phase V_f were determined as a function of time for isothermal treatment. The

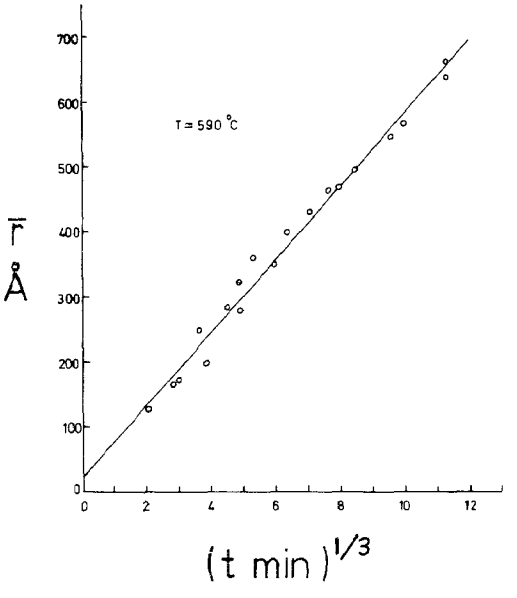

Figure 10 Relationship between mean particle radius and time at 590° C for coarsening of droplets in a 1 K_2O–26 Li_2O–73 SiO_2 (mol %) glass. After McCurrie and Douglas [71].

relations $\bar{r} \propto t^{1/3}$ (Fig. 10), $N_v \propto t^{-1}$, $S_T \propto t^{-1/3}$ and V_f constant were observed, as predicted for diffusion controlled coarsening (it should be remarked that $\bar{r} \propto t^{1/3}$ applied because experimentally $\bar{r} \gg \bar{r}_0$ – see Equation 14). The experimental growth rates for various particle sizes were in good agreement with the theories of Greenwood [62] and Heckel [65].

James and McMillan [72] have also made a detailed study of particle coarsening in a 30 Li_2O–70 SiO_2 (mol %) glass and in Li_2O–SiO_2–P_2O_5 glasses. Instead of replicas, thin samples of phase separated glasses suitable for transmission electron microscopy were prepared from the bulk material by chemical thinning [73]. Stereo pairs of electron micrographs were then used to study directly the three-dimensional distribution of droplets within the thin film, enabling the true size distribution of particles and values of $\bar{r}$, N_v and V_f to be determined from the apparent size distribution on the micrographs. The direct transmission method has the advantage over the replica method of improved resolution, which is particularly useful for studying distributions of finer droplets. The initial separation was essentially complete within a very short period, as in the experiments of Moriya *et al.* [15]. Thereafter the particles coarsened with $\bar{r} \propto t^{1/3}$ and $N_v \propto t^{-1}$, as observed for other compositions. The measured particle size distributions showed some deviations from the Wagner–Lifshitz–Slyozov theory. However, there was very little systematic change in the shapes of the distributions with time suggesting that the steady-state size distribution was achieved at an early stage in the coarsening process.

The phase separation in the P_2O_5 containing glasses exhibited a higher degree of connectivity than in the binary glass (as shown in Fig. 11), although the essential form of the ripening kinetics was not affected by the presence of P_2O_5. The higher connectivity is due to a greater volume fraction of the dispersed silica rich phase, which may be attributed to a raising of the binodal curve of Li_2O–SiO_2 due to P_2O_5 addition [74, 75]. This effect may be due to a tendency of P_2O_5 to associate with Li_2O in the continuous lithia rich phase of these glasses.

Detailed studies of particle coarsening have also been made using small-angle X-ray scattering by Zarzycki [76] in the PbO–B_2O_3 system and by Neilson [77] in the Na_2O–SiO_2 system. In both these studies the particle diameter deduced from SAXS was in accord with Equation 14 for diffusion controlled coarsening.

The kinetics of coarsening of a highly interconnected microstructure have been examined recently by Mahoney *et al.* [78] in a study of the effect of phase separation on the viscosity of a sodium borosilicate glass. To characterize the "scale" of the separation, a "correlation length" Λ

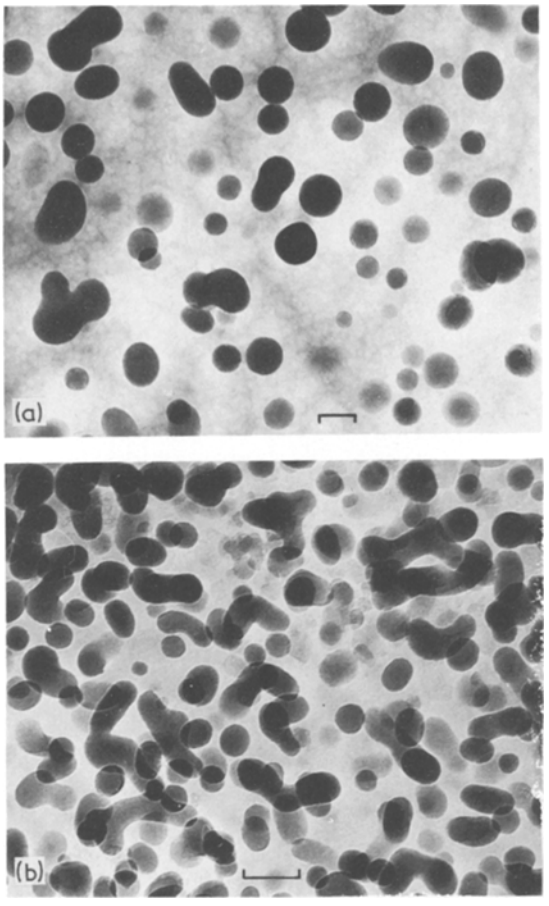

Figure 11 Thin film transmission electron micrographs of (a) 30 Li_2O–70 SiO_2 (mol %) glass heat-treated at 550° C for 16 h, (b) 30 Li_2O–69 SiO_2–1 P_2O_5 glass heat-treated at 550° C for 3 h. Marker indicates 0.1 μm. After James and McMillan [72].

was used, which can be related to the average distance between boundaries $\bar{r}$ measured from electron micrographs ($\Lambda = 0.63\,\bar{r}$). A one third power dependence of $\bar{r}$ (and thus Λ) on heat-treatment time was observed, thus demonstrating experimentally that the kinetics of diffusion controlled coarsening of a highly interconnected microstructure obeys the same power law as for a dispersion of discrete spheres. A similar result was also obtained in the work of Burnett and Douglas [25] to be described shortly.

3.3.3. Kinetics of liquid separation in the soda–lime–silica system

The studies of the commercially important soda–lime–silica system made by Ohlberg and Hammel [68], Hammel [18], Burnett [19] and Burnett and Douglas [25], have been particularly useful in providing information on the kinetics of the early stages of liquid separation. It will be convenient first to consider the work of Burnett and Douglas.

Fig. 12 shows the extent of immiscibility in the soda–lime–silica system as determined by Burnett and Douglas from miscibility temperature

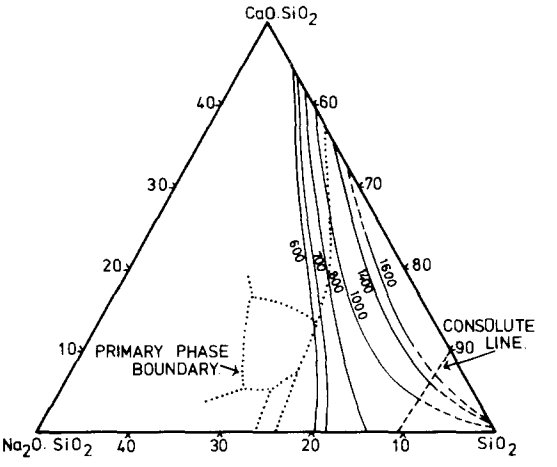

Figure 12 Liquid–liquid immiscibility in the soda–lime–silica system. The isotherms join compositions with the same T_m (° C). After Burnett and Douglas [25].

measurements T_m for compositions ranging from 50 to 85 mol % SiO_2 and from published data for soda–silica and lime–silica (the isotherms join compositions of the same T_m). The miscibility temperatures were obtained by observing the temperatures above which opalescent samples "cleared". The results show good agreement with those of Ohlberg and Hammel [68].

Before embarking on a detailed investigation of the kinetics of separation Burnett and Douglas thoroughly examined the electron microscope replica technique. They observed that the etching time had a pronounced effect on the measured parameters, for example area fraction and number of particles and that excessive etching could introduce serious errors. However, by using a suitable short etching treatment these errors were found to be very small.

Fig. 13 shows the dependence of the morphology of separation on composition. A droplet structure was observed at temperatures just below T_m, i.e. at low supersaturations near the limit of immiscibility. Connected structures were found at high supersaturations after short ageing times (< 20 h), i.e. for compositions and temperatures well within the immiscibility dome. This is the

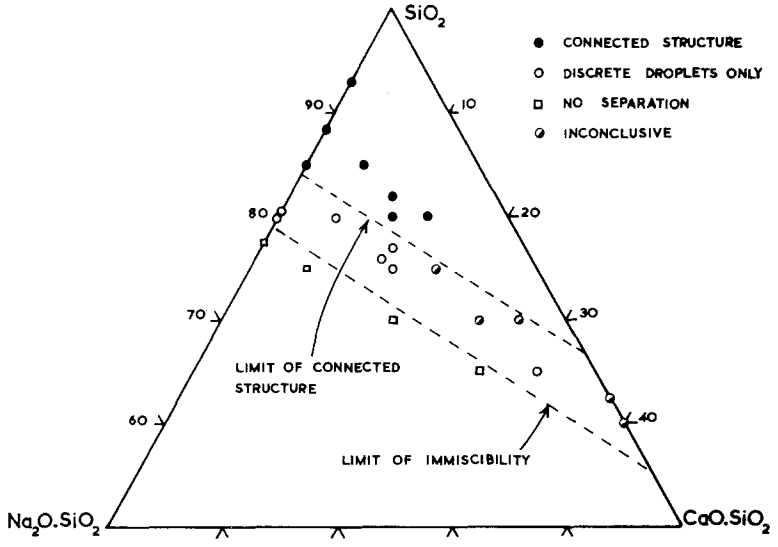

Figure 13 Morphology of liquid-phase separation in the soda–lime–silica system [25]. • connected structure, ○ discrete droplets, □ no separation and ◑ inconclusive.

general behaviour expected from our previous discussion in Section 3.1 but gives no information on the initial mechanism(s). Two compositions were selected for detailed study – glass 80 (80 SiO_2–10 Na_2O–10 CaO mol %) and glass 75 (75 SiO_2–12.5 Na_2O–12.5 CaO) both of which fell on the 1 Na_2O.1 CaO–SiO_2 section of the immiscibility dome (Fig. 14).

Glass 80 was representative of compositions well within the region of immiscibility and just below T_m separated very rapidly into droplets which grew by the coarsening process discussed above with $\bar{r} \propto t^{1/3}$ (Fig. 15a). At lower tempera-

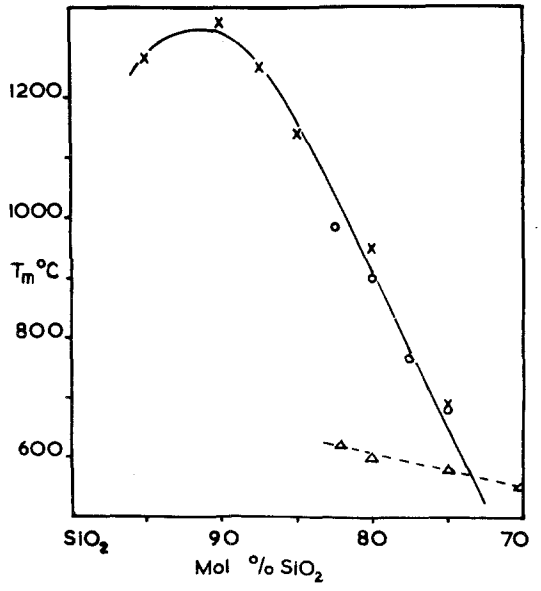

Figure 14 Miscibility gap in the section 1 Na_2O · 1CaO–SiO_2 [25]. ○ experimental values of T_m, × values deduced by interpolation, △ annealing temperature.

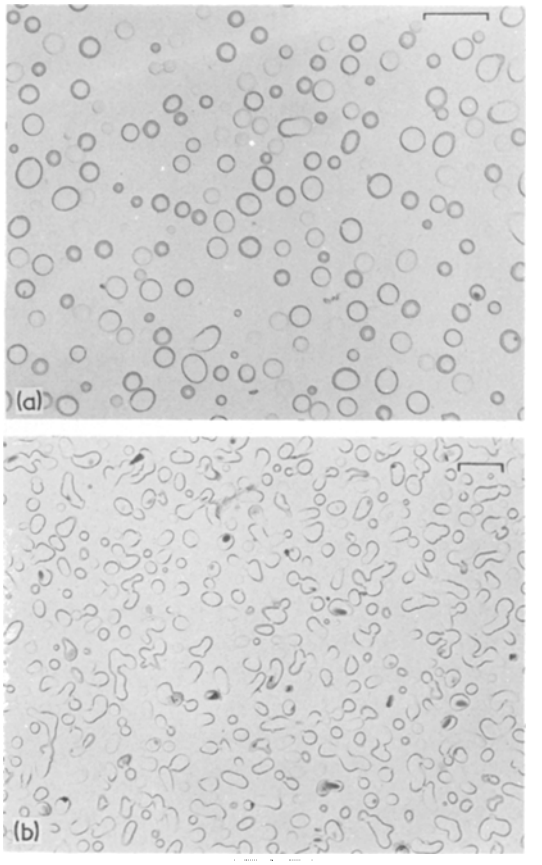

Figure 15 Replica electron micrographs of glass 80 (80 SiO_2–10 Na_2O–10 CaO mol %) heat-treated (a) 740° C for 7.5 h, (b) 660° C for 64 h. Marker indicates 0.5 μm. After Burnett [19].

tures this glass separated into a more connected structure (Fig. 15b). Here the scale of separation was found also to increase with time but the connectivity decreased, showing that the structure was tending towards a configuration of minimum interfacial area, i.e. a collection of spheres. Analysis of the replicas showed that at constant temperature V_f was constant with time but that the interfacial area S_T was proportional to $t^{-1/3}$. According to Haller's analysis (Section 3.2) this indicates coarsening controlled by volume diffusion. It should be noted that $S_T \propto t^{-1/3}$ also held experimentally for the droplet structures suggesting that both connected and droplet phase separation coarsen by a similar diffusion-controlled mechanism.

The T_m for glass 75 was lower than for glass 80 (Fig. 14). Glass 75 separated slowly as droplets enabling the early stages of separation to be studied. Fig. 16 shows the time of heat-treatment necessary to produce the first trace of opalescence in glass 75. In addition to the lower cut off corresponding to the glass transformation temperature T_g there was an upper cut-off below T_m. This indicated the existence of a small upper range of temperature below T_m where nucleation was absent but where particles could still grow (see Section 3.1.1).

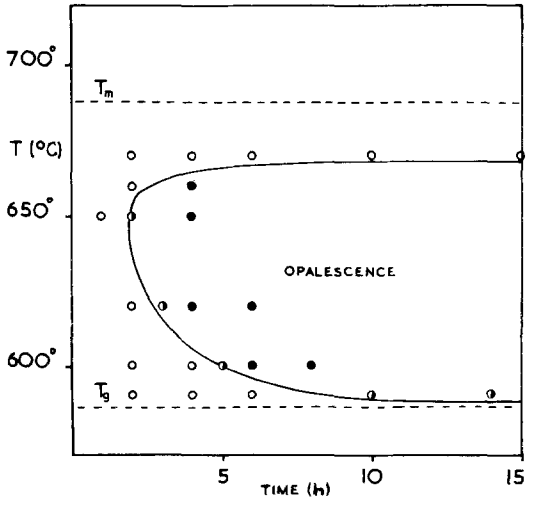

Figure 16 Time of heat-treatment necessary to produce first trace of opalescence in glass 75 ($75SiO_2$–$12.5Na_2O$–12.5 CaO mol %). Note upper cut-off below the miscibility temperature T_m (687° C). • opalescent, ○ clear [25].

Using this fact the rate of nucleation was estimated by heating samples at temperatures within the nucleation range for various times, followed by

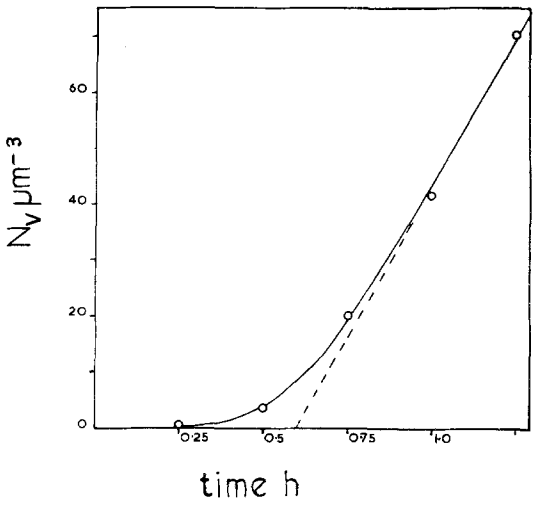

Figure 17 Number of particles per unit volume N_v versus "nucleation time" at 610° C for glass 75. Growth treatment was 675° C for 4 h [25].

heating just below T_m in the upper range to grow the particles nucleated at the lower temperature. Some of the results obtained by electron microscopy are shown in Fig. 17. They indicate that the nucleation rate is not constant but requires a finite induction period before a steady state constant value is achieved. Earlier, Hammel [18] also found non-steady state effects for separation in a $76SiO_2$–$13Na_2O$–11 CaO (mol %) glass. This behaviour arises from the finite time to achieve a steady state concentration of embryos (subcritical size nuclei) and has been treated theoretically [40–42] – Equation 7 above applies to steady state conditions. Owing to the low diffusion rates particularly when approaching the transformation range, such transient effects can be appreciable in glass systems and have been observed also for crystal nucleation [79–82].

The variation of particle radius with time at constant temperature for glass 75 is shown in Fig. 18. Initially the particles grew with $\bar{r} \propto t^{1/2}$ and later $\bar{r} \propto t^{1/3}$ was obeyed. This is as expected for nucleation and diffusion controlled growth followed by coarsening (Section 3.2). In contrast, for glass 80 where separation was more rapid, only the coarsening stage was observed. The onset of coarsening for glass 75 corresponded to an approach to a constant measured volume fraction. The number of particles N_v increased initially due to nucleation but reached a maximum and then decreased due to coarsening.

These growth results have recently been confirmed by Neilson [77] who has studied the early

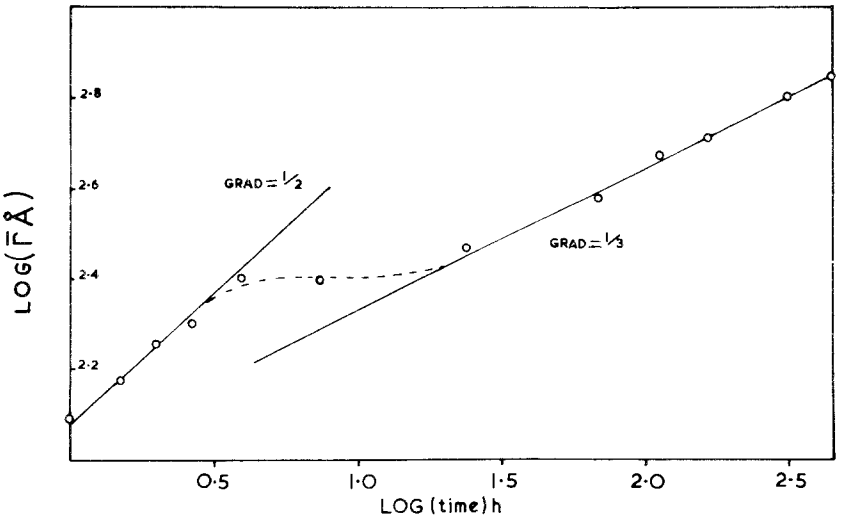

Figure 18 Variation of mean particle radius $\bar{r}$ with time for glass 75 at 640° C [25].

and later stage growth of droplets in a Na_2O–SiO_2 composition using small-angle X-ray scattering.

3.3.4. Metastable region – comparisons with classical theory of homogeneous nucleation

The studies on the soda–lime–silica system indicated that nucleation and growth (as opposed to spinodal decomposition) occurred at low supersaturations, near the immiscibility limit, in qualitative accord with theoretical predictions. Hammel [18] has attempted a quantitative comparison of nucleation theory and experiment, which is in fact [42] one of the few quantitative tests of nucleation (with no adjustable parameters) in condensed systems.

Hammel selected a $76\,SiO_2$–$13\,Na_2O$–$11\,CaO$ (mol%) glass composition near the edge of the miscibility gap where homogeneous nucleation theory should apply. Particle size distributions were obtained from electron micrographs of glass samples heated for various times at temperatures below T_m. Knowing the number and size of particles in a given size interval and their growth rate, the time when the particles were formed was determined by extrapolating back to zero time. Using this method it was possible to obtain nucleation rates (under steady state conditions) at temperatures between 601 and 640° C.

For comparison with theory the values of ΔG_v, σ and ΔG_D were required (Section 3.1.1). ΔG_v was estimated at various undercoolings by fitting the Lumsden solution model [21] to experimental miscibility gap data. A value of $4.6\,mJ\,m^{-2}$ was obtained for σ by measuring the variation of solubility temperature with particle radius. ΔG_D was found from measured particle growth and miscibility gap data, assuming that the diffusion mechanisms involved in nucleation and growth were the same. Fitting these values into Equation 7 the calculated nucleation rates were within an order of magnitude of the experimental results. This is remarkably good agreement but, as pointed out by Hammel, it does not constitute a critical test of the classical theory due to the assumptions made in calculating ΔG_v. Thus the accuracy of the Lumsden model when applied to silicate systems is uncertain and only a small error in the estimated ΔG_v would greatly alter the calculated nucleation rates. In fact another model, the Van der Toorn–Tiedema model [22] gave a larger discrepancy between the theoretical and experimental nucleation rates of between 10 and 10^4, depending on the temperature.

Glass-forming systems are ideal for studying nucleation kinetics experimentally since measurements can be made often very conveniently at the high viscosities and slow diffusion rates involved. However, the lack of accurate thermodynamic data leads to difficulties in assessing nucleation theory quantitatively, and it is relevant to consider the wider evidence available. Recently Heady and Cahn [83] have made a thorough experimental test of classical homogeneous nucleation theory in the C_7H_{14}–C_7F_{14} liquid–liquid miscibility gap system. All the quantities needed to test the theory were accurately determined including the free energy of mixing, phase diagram, surface

tensions and cloud points (where copious nucleation is first observed). A large discrepancy was found between classical theory and experiment for a wide range of initial compositions. Thus the observed undercoolings ΔT below T_m for detectable nucleation were much greater than predicted by theory (typically four times those predicted) – confirming earlier work [84]. It should be mentioned, however, that for initial compositions far from the critical point, theory and experiment appear to be in better agreement.

Heady and Cahn point out that the surprising discrepancy observed cannot be explained by heterogeneous nucleation since this would be expected to give a lower critical undercooling than predicted by classical homogeneous nucleation theory. They were unable to explain the discrepancy by simple modifications of the theory or by considering the diffuse nucleus theory of Cahn and Hilliard [44] and concluded that their result challenged the basis of the classical theory. In another recent study of homogeneous nucleation in a binary fluid mixture of cyclohexane–methanol near the critical point, Huang *et al.* [85] found that the measured critical supercoolings were in good agreement with the predictions of the Cahn and Hilliard theory, as modified by Sarkies and Frankel [86].

Clearly the present evidence is conflicting and further work will be required before the nucleation mechanism in the metastable region of such binary liquid mixtures is completely understood.

3.3.5. Decomposition in the unstable region. Small-angle X-ray scattering results

Small-angle X-ray scattering (SAXS) has so far been the most powerful method for investigating the early stage kinetics in the unstable region and for testing the theory of spinodal decomposition. The striking advantage of the technique [87] is that the diffracted intensity $I(\mathbf{h}, t)$ is proportional to $|A(\boldsymbol{\beta}, t)|^2$, where $\mathbf{h}$ is the scattering vector in reciprocal space ($h = (4\pi/\lambda) \sin\theta/2$ where θ is the scattering angle and λ the wavelength) and $A(\boldsymbol{\beta}, t)$ is the amplitude of the Fourier component of wavenumber $\boldsymbol{\beta}$ at time t. Thus the diffraction spectrum gives directly the distribution of the squares of the amplitudes of the spatial components of the compositional fluctuations. A direct comparison with Cahn's theory may thus be made. The scattering vector $\mathbf{h}$ may be identified with $\boldsymbol{\beta}$ and, for an isotropic system we have

$$I(\beta, t) = I(\beta, 0) \exp(2R(\beta)t). \qquad (15)$$

This equation enables $R(\beta)$ to be determined by measuring the intensity $I(\beta, t)$ as a function of time of heat-treatment. From Equation 13 a plot of $R(\beta)/\beta^2$ versus β^2 should also be linear with a slope of $-2M\kappa$ and an intercept at $\beta^2 = 0$ equal to the interdiffusion coefficient $D(= Mf'')$.

Following the early work of Porai-Koshits and Andreyev [88] a large number of studies have been carried out on phase separated glasses (see for example [89–96]), but here we are mainly concerned with the more recent work on decomposition in the unstable region.

Neilson [95] studied the kinetics of phase separation for two compositions in the Na_2O–SiO_2 system containing 12.6 and 13.2 mol% Na_2O. A temperature range of 450 to 650° C was used, which was well within the miscibility gap (Fig. 3). The initial quench histories of the glasses differed. The 12.6 glass was given a slower quench and had appreciable initial phase separation present before heat-treatment. The intensity versus scattering angle curves for the 12.6 glass when heated at 600° C for times up to 1 h (Fig. 19) yielded a common cross-over point at a given angle (corres-

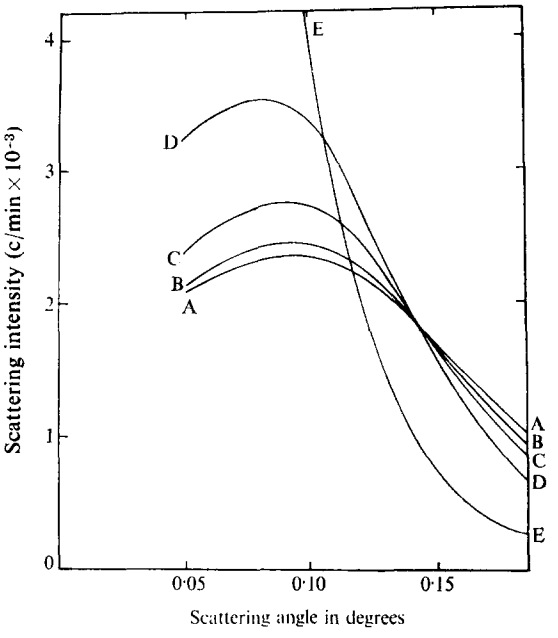

Figure 19 Small-angle X-ray scattering curves for 12.6 mol% Na_2O glass heated at 600° C for following times: A (0 h), B ($\frac{1}{4}$ h), C ($\frac{1}{2}$ h), D (1 h) and E (4 h). After Neilson [95].

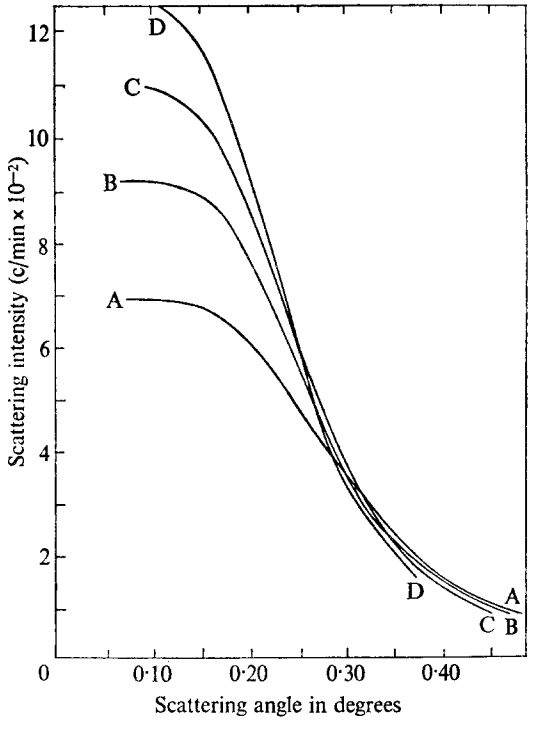

Figure 20 Small-angle X-ray scattering curves for 13.2 mol% Na_2O glass heated at 600° C for following times: A (0 min), B (15 min), C (30 min) and D (45 min). After Neilson [95].

ponding to a given β). This is just the behaviour expected from Cahn's theory. Also the $R(\beta)$ versus β plot at 600° C was in fair agreement with Equation 13 for $\beta < \beta_c$ but some deviation was observed for larger values of β. For longer heat-treatment times when coarsening effects predominated the "cross-over" point shifted to progressively shorter wavenumbers. Again this is as would be expected, at least qualitatively, for the later stages when Cahn's theory no longer holds. In contrast, for the 13.2 mol% Na_2O glass no unique cross-over point was observed even in the early stages of heat-treatment (Fig. 20) in spite of the fact that this glass had been given a more rapid quench than the 12.6 glass and possessed a smaller initial degree of phase separation. Neilson concluded that nucleation and growth was occurring in this glass rather than spinodal decomposition. Certainly appreciable nucleation and growth may have occurred for both glasses since quenching involved crossing the metastable region before the unstable region was reached. Neilson suggested that in the 12.6 glass spinodal decomposition may be occurring simultaneously with the dissolution of particles formed during the cooling, which would be unstable with respect to the spinodal mechanism. This might account for the deviation observed in $R(\beta)$ from theory for $\beta > \beta_c$. An alternative explanation is to be found in the work of Cook [51] on the effect of Brownian motion on spinodal decomposition, as described above.

Tomozawa *et al.* [96] have also studied the kinetics of separation of Na_2O–SiO_2 glasses in the spinodal region. A 13.2 mol% Na_2O glass heat-treated at 560° C gave scattering curves for different heating times which did not exhibit a constant cross-over point, as would be expected from the linearized theory, but the cross-over point shifted to smaller β values as separation proceeded. It was shown that these effects could be explained by the later stage solution given by de Fontaine [97] of Cahn's diffusion equation. It is probable that appreciable phase separation was present in the as-quenched samples.

Both Neilson and Tomozawa *et al.* estimated the interdiffusion coefficient D at different temperatures in the Na_2O–SiO_2 system. The values were in good agreement and were reasonably close to those reported for the diffusion of oxygen anions in silicate glasses. It is interesting to note that Burnett and Douglas [25] in their study of coarsening kinetics in soda–lime–silica also found a diffusion coefficient close to that of oxygen and concluded that oxygen is the rate controlling diffusing species in the phase separation process.

Zarzycki and Naudin [92] examined a 76 B_2O_3–19 PbO–5 Al_2O_3 (wt%) glass, the composition being close to the centre of the immiscibility gap in the ternary system. Rapidly quenched samples were isothermally heat-treated. Analysis of the scattering curves in the initial stage for heat-treatment at 350° C gave a nearly linear $R(\beta)/\beta^2$ versus β^2 plot for $\beta < \beta_c$. Again deviation was observed for higher wavenumbers. No unique cross-over point was observed in the scattered intensity curves. In the initial, short lived, stage the angular position of the maximum was unchanged. At a later stage the maximum shifted to smaller angles, the wavelength corresponding to the intensity maximum varying with time approximately as $t^{1/3}$. This suggested that a coarsening of the highly interconnected microstructure was occurring.

Hopper and Uhlmann [56] have discussed the experimental results for several metallic and glass forming systems in terms of their MFPI formulation of spinodal theory, which essentially takes into account the effect of higher derivative terms

in the diffuse interface expansion. $R(\beta)$ is predicted to decrease less rapidly at large β than in the standard theory. Also in systems in which long range intermolecular forces are important $R(\beta)$ should not be quadratic in β for small β. Qualitatively, this could account for the curvature of the experimental $R(\beta)/\beta^2$ versus β^2 plots – another possible explanation for this effect. However, quantitatively the agreement between theory and experiment was not satisfactory. Hopper and Uhlmann stress the need for more reliable experimental data on initially homogeneous specimens.

Very recently an interesting SAXS study of separation in the B_2O_3–PbO–Al_2O_3 system has been carried out by Srinivasan *et al.* [98]. They point out that both Cahn's theory and its modification by Cook predict a critical wave vector of zero growth and thus a common cross-over point of SAXS curves in the initial stages of decomposition. However, as we have seen, a common cross-over point is not observed in the decomposition studies of quenched samples in the early stages. Srinivasan *et al.* made a theoretical analysis, based on Cook's treatment, for various initial conditions of the specimen prior to treatment at the test (subspinodal) temperature. First they considered the case of a specimen down-quenched from a solution temperature above the immiscibility boundary to the intermediate test temperature, then held for varying times and finally quenched to room temperature. It was found that regardless of the quenching rate no cross-over point should be observed for the early linear growth stages. No detailed discussion can be given here, but this conclusion arises essentially from considering the thermal compositional fluctuations present at both the solution temperature and at lower temperatures. The initial condition at the test temperature is given by the intensity distribution of fluctuations prevalent at the high solution temperature.

The other case discussed by Srinivasan *et al.* was that of up quenching, where the specimen is first quenched from the solution temperature to room temperature and then up quenched to the test or "ageing" temperature. Here a cross-over point may occur, but would mean that decomposition prior to ageing had taken place at a temperature below the test temperature. Analysis of the later stages of decomposition showed that cross-over can also occur with the onset of non-linear growth stages. Srinivasan *et al.* attribute the cross-over observed by previous workers to one or other of these effects. The non-linear stages are also characterized by the appearance of secondary maxima in the scattering intensity curves corresponding to the higher harmonics of the primary spinodal wavelength. These conclusions were supported by a scattering study of the B_2O_3–PbO–Al_2O_3 system using rapidly quenched samples aged at 350° C.

3.3.6. Other evidence

Seward *et al.* [59] have made an electron microscope study of the BaO–SiO_2 system in the region of the miscibility gap. Vapour deposition onto a cold substrate was used to obtain homogeneous glasses and to avoid phase separation due to insufficient quenching. Thin films of the glass were electron-beam heated and the separation process observed directly. For compositions near the centre of the miscibility gap two continuously interconnected phases were observed after separation had occurred. However, at an early stage fine isolated nearly spherical particles were observed, approximately 30 to 50 Å in diameter. This appeared to suggest separation by a nucleation and growth process to produce discrete particles, which then coalesced into an interconnected microstructure, after the mechanism suggested by Haller [57]. The ways in which coalescence may occur have been discussed above (Section 3.1.5). From these results Seward *et al.* emphasize also that observations of final phase separated morphologies are inadequate for specifying the processes by which the morphologies arose.

Other, less direct evidence in support of the Haller model is supplied by the work of MacDowell and Beall [99] on phase separation in Al_2O_3–SiO_2.

An interesting technique recently applied to separation studies involves viscosity measurements. Simmons *et al.* [100] found that a sodium borosilicate composition cooled from a temperature well above the critical temperature T_c to a temperature just below T_c exhibited a significant decrease in viscosity. This was interpreted as evidence that the critical composition of the system separated by nucleation and growth of spheres of the silica-rich phase in the sodium borate-rich phase, instead of by spinodal decomposition. On quenching the same composition to a temperature far below T_c and holding at this temperature the viscosity showed a large increase with time, finally

saturating. This corresponded to the growth and rearrangement of an interconnected structure of the two phases. To explain these results it was suggested that kinetically nucleation may be favoured over spinodal decomposition when the temperature is close to T_c, although spinodal decomposition may be considered more likely thermodynamically. Just below T_c the spinodal mechanism requires large scale compositional fluctuations, although the size of the necessary fluctuations decreases as the temperature is lowered. If the diffusion coefficient is low the formation of these fluctuations takes a long time, and nucleation, which requires only small displacements of the constituents may prevail. Consequently, the spinodal mechanism may be suppressed to lower temperatures.

From much of the discussion it is clear that the kinetics of separation can be influenced by the initial as-quenched state of the sample. Equilibrium composition fluctuations are present even in the single phase region above T_m and may be "frozen in" on rapid quenching to lower temperatures. Zarzycki and Naudin [101] have studied supercritical fluctuations in the liquid B_2O_3–PbO–Al_2O_3 system directly using SAXS and compared the results with quenched glass samples. Also Sarkar *et al.* [102] have shown that fluctuations in the single-phase region of a sodium borosilicate composition can be revealed by replica electron microscopy using a suitable etching treatment. The "size" l of the fluctuations, as assessed by a linear intercept method, was found to vary with temperature according to $1/l^2 \propto (T - T_{sp})$, where T_{sp} is the spinodal temperature, a result indicated by classical fluctuation theory. Estimated values of l in the single phase region just a few degrees above T_m (655° C) were 200 to 300 Å. Measurement of the size of fluctuations above T_m thus provides an independent method of determining the spinodal temperature for a single composition.

3.4. Summary of the kinetics studies

The coarsening process after the initial liquid-phase separation is now reasonably well understood for both droplet and interconnected microstructures.

The observations for temperatures and compositions in the region between the binodal and spinodal boundaries, and in particular close to the binodal, strongly suggest that an homogeneous nucleation mechanism is operative. This is followed by volume diffusion controlled growth of the droplets. Hammel found good quantitative agreement between the experimental nucleation rates and classical theory. However, further quantitative tests of theory have been hampered by the lack of accurate thermodynamic data. Other work, outside glass forming systems, has shown that quantitatively the classical nucleation theory is lacking.

For temperatures and compositions well below the spinodal boundary the evidence in favour of a spinodal decomposition mechanism, in the early stages of separation, is accumulating. In much of the earlier small-angle X-ray scattering work the specimens studied had already separated to a large extent during quenching from above the miscibility gap, prior to isothermal holding below the spinodal. Consequently, the very early stages of separation were not observed. However, decomposition of the most rapidly quenched samples showed disagreement with Cahn's linearized theory. Recent theoretical work has demonstrated that this disagreement may be attributed to neglect of various non-linear terms in the formulation and also neglect of random thermal fluctuations. The inclusion of thermal fluctuations in the theory appears particularly promising in reconciling theory and experiment. Future theoretical analysis will need to take into account both the non-linear effects and thermal fluctuations, and recent work has been in this direction [103]. On the experimental side future work will require careful choice of systems and rapid quenching techniques, perhaps including splat quenching and vapour deposition, to ensure that no significant separation occurs prior to isothermal holding.

In spite of the recent SAXS evidence in support of a spinodal decomposition mechanism certain reservations remain. Thus the impressive electron microscopy of Seward *et al.* [59] on BaO–SiO_2 glasses suggests that nucleation and growth may be occurring for a composition within the spinodal region. One problem, however, with the electron microscopy of very fine scale phase separation is that it can be difficult to decide whether very fine dots of <50 Å diameter are really discrete particles with relatively sharp interfaces or are more gradual compositional fluctuations. Furthermore, morphological observations, even when recorded as a function of time can be of limited value in deciding the mechanism, particularly if the holding temperature is not far below the

spinodal [43]. In this case fluctuations rapidly sharpen and begin to coarsen and the process is not easily distinguished from a nucleation and growth process.

It is now clear that high interconnectivity in the later stages of separation is not a sufficient criterion for spinodal decomposition but may arise also from nucleation and intersecting growth.

As yet a possibility which cannot be discounted is that the effective spinodal boundary in some systems may be depressed to lower temperatures even in the vicinity of the critical point [100]. Thus samples quenched from above T_c would always have to traverse a nucleation region before reaching the spinodal and very rapid quenching would be required to suppress prior nucleation.

Another question remains to be answered concerning the scattering techniques. As pointed out by Goldstein [104] the existence of a maximum in the scattered intensity for a given angle with the intensity falling to zero at zero scattering angle, as predicted by spinodal theory, is also predicted in general form by a nucleation and growth mechanism with the particles surrounded by a diffusion depleted region. Wright [105] has also shown that the shape alone of X-ray or neutron scattering curves cannot be taken as a sufficient criterion for spinodal decomposition. Further detailed theoretical investigation of the scattering problem for nucleation and growth is still required. This question has been discussed recently [106–108].

In conclusion, we feel that there is reasonable evidence at present for both spinodal decomposition and nucleation, under the appropriate conditions. For the future it is hoped that the observations discussed will be reconciled within the framework of an unified theory which treats spinodal decomposition and nucleation and growth as limiting cases, and includes the "no theory" region in the vicinity of the spinodal, as suggested by Hilliard [43] and Cook [51]. Experimentally there is scope for further refined scattering studies in close conjunction with high resolution electron microscopy of replicas and thin sections in order to answer the outstanding questions.

4. Effect of phase separation on crystallization and on glass properties

One area which is not fully understood is the relationship between liquid-phase separation in glasses and crystal nucleation and growth. It is well known from phase-diagram data that prior phase separation can influence the course of crystallization in a system. Thus liquid unmixing may produce two compositions one of which is more prone to crystallize than the initial unseparated glass [109, 110]. There are other possible effects which, as yet, are not well established experimentally. Thus Cahn [111] has shown that in a system tending to phase separate the driving force for crystallization may be increased or decreased, and in some cases crystallization may be thermodynamically blocked until liquid separation has occurred. It has also been suggested that droplet interfaces may act as preferred sites for crystal nucleation, but apart from the work of Ohlberg *et al.* [112] there is so far little evidence in general support of this mechanism. These and other possible effects have been discussed in detail [9, 113, 114].

Following the extensive work on the mechanism and kinetics of phase separation, increasing attention has been directed in recent years to the effects of phase separation on physical and chemical properties. We will give only an outline of these effects (for details see [115–141]). Properties that have been studied include density [115, 117, 118], thermal expansion [116, 117], elastic properties [115–117], strength [126–128], internal friction [119–122], electrical conductivity [119, 123–125] and viscosity [78, 100, 129–134]. A valuable source of Russian data is the "Structure of Glass" series (Volume 8 is devoted to phase-separation phenomena [8]).

Shaw and Uhlmann [115] have analysed the variation of density and elastic moduli with composition across a miscibility gap for a number of binary glass systems. Plots of density versus composition in wt % have a positive (concave upward) curvature across a two phase region. This provides a useful method of detecting suspected phase separation in certain glass systems.

The temperature dependence of elastic moduli and thermal expansion of soda–silica glasses [116] were found to be greatly influenced by the amount and distribution of phase separation. Glasses with two independently interconnected phases tended to be more rigid than homogeneous glasses with the same nominal composition. The properties of glasses having particles dispersed in a continuous matrix were determined primarily by the continuous phase.

Phase separation in soda–silica glasses [119] and mixed alkali silicate glasses [120] had little effect on the internal friction. This was attributed to the short range of the ionic transport processes involved in internal friction compared with the scale of the separated phases. Mazurin [121], however, has reported an internal friction peak in a sodium borosilicate composition which may be due to separation of the highly viscous continuous phase. In contrast the d.c. electrical conductivity, which involves the transport of charged ions over larger distances can be greatly affected by separation. Thus, in general, the conductivity is determined by the high conductivity phase if this phase is continuous, and by the low conductivity phase if the high conductivity phase is discontinuous.

The strength of phase-separated glasses as measured by modulus of rupture and ball indentation [126, 127] decreased with increase in the scale of separation. However, an initial rise in strength has been observed [128] for the very early stage of separation when two fine scale interconnected phases are formed.

A number of recent studies on silicate and borosilicate glasses have shown a pronounced effect of phase separation on viscosity. The viscosity of a separated glass depends, for example, on whether the high viscosity phase is continuous or discontinuous [129, 130]. Large increases of viscosity of up to five orders of magnitude have been observed during separation at constant temperatures. For a sodium borosilicate composition which separated into two interconnected phases the large viscosity increase was attributed to the growth in size of the viscous phase during the coarsening or rearrangement stage [78]. The time dependence of viscosity ("viscosity drift") has been used to detect the presence of phase separation in glasses [134] and to measure T_m – a method which appears to be convenient for systems with low temperature miscibility gaps.

It is interesting to note that the double glass transition due to the two phases in a glass has been observed in a chalcogenide system [135] using heat capacity measurements versus temperature. Isotherms of glass transformation temperature have been used to determine tie line directions in the immiscibility region of the ternary Na_2O–B_2O_3–SiO_2 system [136].

Finally, some mention should be made of the important property of chemical durability. Work on phase separated glasses dates back to the pioneering study of Turner and Winks [137] on borosilicate glasses, which was followed by the development of the Vycor process [138]. We make no attempt to give a full list of references on this subject but offer references [139–141] for further details.

Further fundamental studies of the processes of phase separation in glasses and studies of the properties of phase separated glasses will certainly continue to be of great importance to both glass and glass-ceramic technologies.

Acknowledgements

Thanks are due to the following authors and bodies for permission to reproduce illustrations and micrographs: Professor R. W. Douglas, Dr G. F. Neilson, The Society of Glass Technology (for Figs. 10 to 14 inclusive and Figs. 16 to 20 inclusive), Professor J. W. Cahn and *Metallurgical Transactions* for Fig. 9 (modified from Fig. 9 J. W Cahn *Trans. Met. Soc. AIME* 242 (1968) 166).

References

1. J. W. GREIG, *Amer. J. Sci.* 13 (1927) 1, 133.
2. H. RAWSON, "Inorganic Glass-Forming Systems" Academic Press, London, 1967).
3. S. D. STOOKEY, Corning Glass Works, U.S. Patent 2,920,971 (1/12/1960).
4. P. W. MCMILLAN, "Glass Ceramics" (Academic Press, London, 1964).
5. E. M. LEVIN, "Phase Diagrams", Vol. 3, edited by A. M. Alper (Academic Press, London, 1970) p. 143.
6. F. YA. GALAKHOV and B. G. VARSHAL, in "The Structure of Glass," edited by E. A. Porai-Koshits, (Consultants Bureau, New York, 1973) Vol. 8, p. 7.
7. J. W. CAHN and R. J. CHARLES, *Phys. Chem. Glasses* 6 (1965) 181.
8. E. A. PORAI-KOSHITS, ED, "The Structure of Glass", Vol. 8, see [6].
9. T. P. SEWARD III, "Phase Diagrams", Vol. 1, edited by A. M. Alper (Academic Press, London, 1970) p. 295.
10. A. H. COTTRELL, "Theoretical Structural Metallurgy" (Arnold, London, 1948) p. 139.
11. J. H. HILDEBRAND, *J. Amer. Chem. Soc.* 51 (1929) 66.
12. J. B. THOMSON JUN., "Researches in Geochemistry" Vol. 2, edited by P. H. Abelson (John Wiley, New York, 1967) p. 340.
13. L. S. DARKEN and R. W. GURRY, "Physical Chemistry of Metals" (McGraw Hill, New York, 1953).
14. R. J. CHARLES, *J. Amer. Ceram. Soc.* 50 (1967) 631.
15. Y. MORIYA, D. H. WARRINGTON and R. W. DOUGLAS, *Phys. Chem. Glasses* 8 (1967) 19.

16. N. S. ANDREEV, D. A. GOGANOV, E. A. PORAI-KOSHITS and Y. G. SOKOLOV, in "The Structure of Glass", Vol. 3, edited by E. A. Porai-Koshits (Consultants Bureau, New York, 1964) p. 47.
17. W. HALLER, D. H. BLACKBURN and J. H. SIMMONS, *J. Amer. Ceram. Soc.* **57** (1974) 120.
18. J. J. HAMMEL, *J. Chem. Phys.* **46** (1967) 2234.
19. D. G. BURNETT, Ph.D. thesis, University of Sheffield (1968).
20. H. K. HARDY, *Acta Met.* **1** (1953) 202.
21. J. LUMSDEN, "Thermodynamics of Alloys" (Institute of Metals, London, 1952).
22. L. J. VAN DER TOORN and T. J. TIEDEMA, *Acta Met.* **8** (1960) 711.
23. D. DE FONTAINE and J. E. HILLIARD, *ibid* **13** (1965) 1019.
24. H. E. COOK and J. E. HILLIARD, *Trans. Met. Soc. AIME* **233** (1965) 142.
25. D. G. BURNETT and R. W. DOUGLAS, *Phys. Chem. Glasses* **11** (1970) 125.
26. B. E. WARREN and A. G. PINCUS, *J. Amer. Ceram. Soc.* **23** (1940) 301.
27. A. DIETZEL, *Glastech. Ber.* **22** (1948) 41, 81; *ibid* **22** (1949) 212.
28. E. M. LEVIN and S. BLOCK, *J. Amer. Ceram. Soc.* **40** (1957) 95, 113.
29. H. RAWSON, in [2] p. 121.
30. R. J. CHARLES, *Phys. Chem. Glasses* **10** (1969) 169.
31. F. D. RICHARDSON, *Discuss. Faraday Soc.* **4** (1948) 244.
32. J. D. MACKENZIE, "Modern aspects of the vitreous state", Vol. 1, (Butterworths, London, 1960) p. 1.
33. C. R. MASSON, *Proc. Roy. Soc. A* **287** (1965) 201; *J. Iron Steel Inst.* **210** (1972) 89.
34. I. PRIGOGINE and R. DEFAY, "Chemical Thermodynamics" (Longmans, London, 1962) p. 418.
35. Y. MORIYA, *Rep. Govt. Ind. Res. Inst., Osaka, Japan,* **339** (1971) 24.
36. F. LIEBAU, *Acta Cryst.* **14** (1961) 389.
37. P. B. MACEDO and J. H. SIMMONS, *J. Res. Nat. Bur. Stand. A* **78** (1974) 53.
38. R. R. SHAW and D. R. UHLMANN, *J. Amer. Ceram. Soc.* **51** (1968) 377.
39. J. H. SIMMONS, *ibid* **56** (1973) 284.
40. J. W. CHRISTIAN, "The Theory of Phase Transformations in Metals and Alloys" (Pergamon Press, London, 1965).
41. A. C. ZETTLEMOYER, ED., "Nucleation" (Marcel Dekker, New York, 1969).
42. K. C. RUSSEL, in "Phase Transformations", edited by H. I. Aronson (Amer. Soc. Metals, distributed by Chapman and Hall, London, 1970) p. 219.
43. J. E. HILLIARD, in [42] p. 497.
44. J. W. CAHN and J. E. HILLIARD, *J. Chem. Phys.* **28** (1958) 258; *ibid* **31** (1959) 688.
45. J. W. GIBBS, "The Scientific Papers of J. W. Gibbs" (Dover, New York, 1961).
46. M. HILLERT, D.Sc. thesis, Massachusetts Institute of Technology (1956); *Acta Met.* **9** (1961) 525.
47. J. W. CAHN, *Acta Met.* **9** (1961) 795.
48. *Idem, J. Chem. Phys.* **42** (1965) 93; *Trans. Met. Soc. AIME* **242** (1968) 166.
49. *Idem, Acta Met.* **14** (1966) 1685.
50. J. E. HILLIARD, in [42] p. 528.
51. H. E. COOK, *Acta Met.* **18** (1970) 297.
52. J. E. HILLIARD, in [42] p. 554.
53. R. W. HOPPER and D. R. UHLMANN, *J. Chem. Phys.* **56** (1972) 4043.
54. *Idem, Acta Met.* **21** (1973) 267.
55. *Idem, ibid* **21** (1973) 35.
56. *Idem, ibid* **21** (1973) 377.
57. W. HALLER, *J. Chem. Phys.* **42** (1965) 686.
58. M. GOLDSTEIN, *J. Crystal Growth* **3** (1968) 594.
59. T. P. SEWARD III, D. R. UHLMANN and D. TURNBULL, *J. Amer. Ceram. Soc.* **51** (1968) 634.
60. W. HALLER and P. B. MACEDO, *Phys. Chem. Glasses* **9** (1968) 153.
61. R. W. HOPPER and D. R. UHLMANN, *Discuss. Faraday Soc.* **50** (1970) 166.
62. G. W. GREENWOOD, *Acta Met.* **4** (1956) 243.
63. C. WAGNER, *Z. Elektrochem.* **65** (1961) 581.
64. I. M. LIFSHITZ and V. V. SLYOZOV, *J. Phys. Chem. Solids* **19** (1961) 35.
65. R. W. HECKEL, *Trans. Met. Soc. AIME* **233** (1965) 1994.
66. S. M. OHLBERG, and H. R. GOLOB, *J. Amer. Ceram. Soc.* **48** (1965) 178.
67. S. M. OHLBERG, H. R. GOLOB, J. J. HAMMEL and R. R. LEWCHUK, *ibid* **48** (1965) 331.
68. S. M. OHLBERG and J. J. HAMMEL, 7th International Congress on Glass, Brussels (1965) paper 32.
69. J. J. HAMMEL and S. M. OHLBERG, *J. Appl. Phys.* **36** (1965) 1442.
70. M. GOLDSTEIN, *ibid* **34** (1963) 1928.
71. R. A. MCCURRIE and R. W. DOUGLAS, *Phys. Chem. Glasses* **8** (1967) 132.
72. P. F. JAMES and P. W. MCMILLAN, *ibid* **11** (1970) 59; *ibid* **11** (1970) 64.
73. *Idem, Phil. Mag.* **18** (1968) 863.
74. Y. MORIYA, in [35] p. 48.
75. M. TOMOZAWA, in "Advances in Nucleation and Crystallization in Glasses" (Amer. Ceram. Soc., Columbus, Ohio, 1971) p. 41.
76. J. ZARZYCKI and F. NAUDIN, *Phys. Chem. Glasses* **8** (1967) 11.
77. G. F. NEILSON, *ibid* **13** (1972) 70.
78. R. MAHONEY, G. R. SRINIVASAN, P. B. MACEDO, A. NAPOLITANO and J. H. SIMMONS, *ibid* **15** (1974) 24.
79. D. G. BURNETT and R. W. DOUGLAS, *ibid* **12** (1971) 117.
80. Z. STRNAD and R. W. DOUGLAS, *ibid* **14** (1973) 33.
81. V. N. FILIPOVITCH and A. M. KALININA, *Neorg. Mater.* **4** (1968) 1532; *ibid* **6** (1970) 351; *ibid* **7** (1971) 1844
82. P. F. JAMES, *Phys. Chem. Glasses* **15** (1974) 95.
83. R. B. HEADY and J. W. CAHN, *J. Chem. Phys.* **58** (1973) 896.
84. B. E. SUNDQUIST and R. A. ORIANI, *Trans. Faraday Soc.* **63** (1967) 561.

85. J. S. HUANG, S. VERNON and N. C. WONG, *Phys. Rev. Letters* **33** (1974) 140.
86. K. W. SARKIES and N. E. FRANKEL, *J. Chem. Phys.* **54** (1971) 433.
87. K. B. RUNDMAN and J. E. HILLIARD, *Acta Met.* **15** (1967) 1025.
88. E. A. PORAI-KOSHITS and N. S. ANDREYEV, *Nature* **182** (1958) 336; *J. Soc. Glass Techn.* **43** (1959) 235T.
89. E. A. PORAI-KOSHITS, D. A. GOGANOV and V. I. AVERJANOV, "Physics of non-crystalline solids" (North Holland, Amsterdam, 1965) p. 117.
90. J. A. WILLIAMS, B. PHILLIPS, G. E. RINDONE and H. A. MCKINSTRY, "Advances in X-ray analysis", Vol. 8 (Plenum Press, New York, 1965) p. 59.
91. N. S. ANDREYEV and E. A. PORAI-KOSHITS, *Discuss. Faraday Soc.* **50** (1970) 135.
92. J. ZARZYCKI and F. NAUDIN, *J. Non-Cryst. Solids* **1** (1969) 215.
93. J. ZARZYCKI, *Discuss. Faraday Soc.* **50** (1970) 122.
94. G. F. NEILSON, *ibid* **50** (1970) 145.
95. *Idem, Phys. Chem. Glasses* **10** (1969) 54.
96. M. TOMOZAWA, R. K. MACCRONE and H. HERMAN, *ibid* **11** (1970) 136.
97. D. DE FONTAINE, Ph.D. thesis, Northwestern University (1967).
98. G. R. SRINIVASAN, R. COLELLA, P. B. MACEDO and V. VOLTERRA, *Phys. Chem. Glasses* **14** (1973) 90.
99. J. F. MACDOWELL and G. H. BEALL, *J. Amer. Ceram. Soc.* **52** (1969) 17.
100. J. H. SIMMONS, P. B. MACEDO, A. NAPOLITANO and W. K. HALLER, *Discuss. Faraday Soc.* **50** (1970) 155.
101. J. ZARZYCKI and F. NAUDIN, *J. Non-Cryst. Solids* **5** (1971) 415.
102. A. SARKAR, G. R. SRINIVASAN, V. VOLTERRA and P. B. MACEDO, *Phys. Chem. Glasses* **14** (1973) 114.
103. J. S. LANGER, *Acta Met.* **21** (1973) 1649.
104 M. GOLDSTEIN, *Discuss. Faraday Soc.* **50** (1970) 224
105. A C. WRIGHT, *ibid* **50** (1970) 111.
106. P. K GUPTA and A. R. COOPER, in [75] p. 24.
107. D. T. STURGILL, in [75] p. 33.
108. D. T. STURGILL and R. J. STUBLER, *Amer. Ceram. Soc. Bull.* **52** (1974) 382.
109. H. HARPER, P. F. JAMES and P. W. MCMILLAN, *Discuss. Faraday Soc.* **50** (1970) 206.
110. D. G. BURNETT and R. W. DOUGLAS, *ibid* **50** (1970) 200.
111. J. W. CAHN, *J. Amer. Ceram. Soc.* **52** (1969) 118.
112. S. M. OHLBERG, H. R. GOLOB and D. W. STRICKLER, in "Symposium on Nucleation and Crystallization in Glasses and Melts" edited by M. K. Reser, G. Smith and H. Insley (Amer. Ceram. Soc., Columbus, Ohio, 1962) p. 55.
113. J. J. HAMMEL, in [75] p. 1.
114. M. TOMOZAWA, *Phys. Chem. Glasses* **13** (1972) 161; *ibid* **14** (1973) 112.
115. R. R. SHAW and D. R. UHLMANN, *J. Non-Cryst. Solids* **1** (1969) 474; *ibid* **5** (1971) 237.
116. R. H. REDWINE and M. B. FIELD, *J. Mater. Sci.* **3** (1968) 380.
117. L. D. PYE, L. PLOETZ and L. MANFREDO, *J. Non-Cryst. Solids* **14** (1974) 310.
118. S. P. ZHDANOV, E. V. KOROMALDI and L. G. SMIRNOVA, Proceedings of the 9th International Congress on Glass (Institut Du Verre, Versailles, 1971) Vol. 1, p. 463.
119. R. H. REDWINE and M. B. FIELD, *J. Mater Sci.* **4** (1969) 713.
120. S. W. TAYLOR and D. E. DAY, *Phys. Chem. Glasses* **11** (1970) 89.
121. O. V. MAZURIN, *ibid* **9** (1968) 165.
122. P. JA. BOKIN, F. JA. GALAKHOV and E. N. STEPANOV, Proceedings of the 9th International Congress on Glass (Institut Du Verre, Versailles, 1971) Vol. 1, p. 335.
123. R. J. CHARLES, *J. Amer. Ceram. Soc.* **46** (1963) 235; *ibid* **49** (1966) 55.
124. S. V. PHILLIPS and P. W. MCMILLAN, *Glass Technol.* **6** (1965) 46.
125. P. M. HAKIM and D. R. UHLMANN, *Phys. Chem. Glasses* **12** (1971) 132.
126. Y. UTSUMI, S. SAKKA and M. TASHIRO, *Glass Technol* **11** (1970) 80.
127. Y. UTSUMI and S. SAKKA, *ibid* **11** (1970) 86.
128. D. F. USHAKOV, A. I. KUZNETSOV and E. M. MILYUKOV, *Inorganic Mats.* **6** (1970) 1785.
129. O. V. MAZURIN, G. P. ROSKOVA and V. P. KLUYEV, *Discuss. Faraday Soc.* **50** (1970) 191.
130. J. H. LI and D. R. UHLMANN, *J. Non-Cryst. Solids* **3** (1970) 205.
131. O. V. MAZURIN, V. P. KLUYEV and G. P. ROSKOVA, *Phys. Chem. Glasses* **11** (1970) 192.
132. P. BERNHEIM and A. C. D. CHAKLADER, *J. Non-Cryst. Solids* **5** (1971) 328.
133. J. H. SIMMONS, S. A. MILLS and A. NAPOLITANO, *J. Amer. Ceram. Soc.* **57** (1974) 109; *J. Non-Cryst. Solids* **14** (1974) 302.
134. W. HALLER, J. H. SIMMONS and A. NAPOLITANO, *J. Amer. Ceram. Soc.* **54** (1971) 299.
135. C. T. MOYNIHAN, P. B. MACEDO, I. D. AGGARWAL and U. E. SCHNAUS, *J. Non-Cryst. Solids* **6** (1971) 322.
136. O. V. MAZURIN and M. V. STRELTSINA, *ibid* **11** (1972) 199. (See also comments by S. SCHOLES, *J. Non-Cryst. Solids* **12** (1973) 266.)
137. W. E. S. TURNER and F. WINKS, *J. Soc. Glass Technol.* **10** (1926) 102.
138. H. P. HOOD and M. E. NORDBERG, US Patent 2,106,744 (1934).
139. M. B. VOLF, "Technical Glasses", (Pitman, London, 1961) pp. 176–209.
140. E. M. LEVIN, as in [5] p. 244.
141. N. P. DANILOVA, O. V. MAZURIN and T. S. TSEKHOMSKAYA, Proceedings of the 9th International Congress on Glass (Institut Du Verre, Versailles, 1971) Vol. 1, p. 825.

Received 22 April and accepted 13 May 1975.